LAWRENCE
LIVERMORE
NATIONAL
LABORATORY

LLNL-JRNL-402271

A multi-model assessment of pollution transport to the Arctic

D. T. Shindell, M. Chin, F. Dentener, R. M. Doherty, G. Faluvegi, A. M. Fiore, P. Hess, D. M. Koch, I. A. MacKenzie, M. G. Sanderson, M. G. Schultz, M. Schulz, D. S. Stevenson, H. Teich, C. Textor, O. Wild, D. J. Bergmann, I. Bey, H. Bian, C. Cuvelier, B. N. Duncan, G. Folberth, L. W. Horowitz, J. Jonson, J. W. Kaminski, E. Marmer, R. Park, K. J. Pringle, S. Schroeder, S. Szopa, T. Takemura, G. Zeng, T. J. Keating, A. Zuber

March 14, 2008

Atmospheric Chemistry and Physics Discussions

Disclaimer

A multi-model assessment of pollution transport to the Arctic

D. T. Shindell[1], M. Chin[2], F. Dentener[3], R. M. Doherty[4], G. Faluvegi[1], A. M. Fiore[5], P. Hess[6], D. M. Koch[1], I. A. MacKenzie[4], M. G. Sanderson[7], M. G. Schultz[8], M. Schulz[9], D. S. Stevenson[4], H. Teich[1], C. Textor[9], O. Wild[10], D. J. Bergmann[11], I. Bey[12], H. Bian[13], C. Cuvelier[3], B. N. Duncan[13], G. Folberth[12], L. W. Horowitz[5], J. Jonson[14], J. W. Kaminski[15], E. Marmer[3], R. Park[16], K. J. Pringle[7,*], S. Schroeder[8], S. Szopa[9], T. Takemura[17], G. Zeng[18], T. J. Keating[19], A. Zuber[20]

[1]{NASA Goddard Institute for Space Studies and Columbia University, New York, NY, USA}
[2]{NASA Goddard Space Flight Center, Greenbelt, MD, USA}
[3]{European Commission, Institute for Environment and Sustainability, Joint Research Centre, Ispra, Italy}
[4]{School of GeoSciences, University of Edinburgh, UK}
[5]{NOAA Geophysical Fluid Dynamics Laboratory, Princeton, NJ, USA}
[6]{National Center for Atmospheric Research, Boulder, CO, USA}
[7]{Met Office Hadley Centre, Exeter, UK}
[8]{ICG-2, Forschungszentrum-Jülich, Germany}
[9]{Laboratoire des Science du Climat et de l'Environnement, Gif-sur-Yvette, France}
[10]{Department of Environmental Science, Lancaster University, UK}
[11]{Atmospheric Science Division, Lawrence Livermore National Laboratory, CA, USA}
[12]{Laboratoire de Modélisation de la Chimie Atmosphérique, Ecole Polytechnique Fédérale de Lausanne, Lausanne, Switzerland}
[13]{Goddard Earth Science & Technology Center, U. Maryland Baltimore County, MD, USA}

[14]{Norwegian Meteorological Institute, Oslo, Norway}
[15]{Center for Research in Earth and Space Science, York University, Canada}
[16]{Atmospheric Chemistry Modeling Group, Harvard University, Cambridge, MA, USA and School of Earth and Environmental Sciences, Seoul National University, Seoul, Korea}
[17]{Research Institute for Applied Mechanics, Kyushu University, Japan}
[18]{National Centre for Atmospheric Science, Department of Chemistry, University of Cambridge, Cambridge, UK}
[19]{Office of Policy Analysis and Review, Environmental Protection Agency, Washington DC, USA}
[20]{Environment Directorate General, European Commission, Brussels, Belgium}
[*]{now at: Max Planck Institute for Chemistry, Mainz, Germany}
Correspondence to: D. T. Shindell (dshindell@giss.nasa.gov)

Abstract

We examine the response of Arctic gas and aerosol concentrations to perturbations in pollutant emissions from Europe, East and South Asia, and North America using results from a coordinated model intercomparison. These sensitivities to regional emissions (mixing ratio change per unit emission) vary widely across models and species. Intermodel differences are systematic, however, so that the relative importance of different regions is robust. North America contributes the most to Arctic ozone pollution. For aerosols and CO, European emissions dominate at the Arctic surface but East Asian emissions become progressively more important with altitude, and are dominant in the upper troposphere. Sensitivities show strong seasonality: surface sensitivities typically maximize during boreal winter for European and during spring for East Asian and North American emissions. Mid-tropospheric sensitivities, however, nearly always maximize during spring or summer for all regions. Deposition of black carbon (BC) onto Greenland is most sensitive to North American emissions. North America and Europe each contribute ~40% of total BC deposition to Greenland, with ~20% from East Asia.

Elsewhere in the Arctic, both sensitivity and total BC deposition are dominated by European emissions. Model diversity for aerosols is especially large, resulting primarily from differences in aerosol physical and chemical processing (including removal). Comparison of modeled aerosol concentrations with observations indicates problems in the models, and perhaps, interpretation of the measurements. For gas phase pollutants such as CO and O_3, which are relatively well-simulated, the processes contributing most to uncertainties depend on the source region and altitude examined. Uncertainties in the Arctic surface CO response to emissions perturbations are dominated by emissions for East Asian sources, while uncertainties in transport, emissions, and oxidation are comparable for European and North American sources. At higher levels, model-to-model variations in transport and oxidation are most important. Differences in photochemistry appear to play the largest role in the intermodel variations in Arctic ozone sensitivity, though transport also contributes substantially in the mid-troposphere.

1 Introduction

Transport of pollution to the Arctic affects both air quality and climate change. While levels of pollutants such as tropospheric ozone and aerosols are generally lower in the Arctic than in industrialized areas, they can have substantial impacts on climate. For example, aerosols can greatly perturb the Arctic radiation balance (Garrett and Zhao, 2006; Lubin and Vogelmann, 2006). Though pollutant levels outside the Arctic may in fact have a larger influence than local pollutant levels on Arctic climate (Shindell, 2007), at least for historical changes, it is important to understand the sources of the pollution that reaches the Arctic. This pollution alters local radiative fluxes, temperature profiles and cloud properties. Pollutant levels within the Arctic are especially important for climate in the case of black carbon (BC), which clearly has a strong local climate impact when it is deposited onto snow and ice surfaces, reducing their albedo (Hansen and Nazarenko, 2004; Jacobson, 2004; Warren and Wiscombe, 1980; Vogelmann et al., 1988).

While air pollution in most heavily populated areas of the world comes predominantly from local and regional emissions, pollution in the remote Arctic is primarily a result of

long-range transport from source regions outside the Arctic. Pollution can be transported to the Arctic along a variety of pathways, with transport at low levels followed by uplift or diabatic cooling and tranport at high altitudes following uplift near the emission source regions seen in a Langrangian model (Stohl, 2006). While there is general support for large contributions to Arctic pollution from both Eurasian and North American emissions (Xie et al., 1999; Sharma et al., 2006), it is crucial to quantify the relative importance of emissions from various source regions in determining local pollutant levels (Stohl, 2006). This will enable us to better understand the influence of past emission changes, such as the apparent maximum in North American BC emissions in the early 20th century (McConnell et al., 2007), and future changes such as the expected continuing decrease in emissions from mid/high latitude developed nations while emissions from lower latitude developing nations increase. Additionally, it will help to inform potential strategies to mitigate Arctic warming via short-lived pollutants (Quinn et al., 2007).

In this paper, we examine model simulations performed within the Task Force on Hemispheric Transport of Air Pollution (HTAP), a project to develop a fuller understanding of long-range transport of air pollution in support of the 51-nation Convention on Long-Range Transboundary Air Pollution. Using these simulations, we can analyze transport of a variety of idealized and actual pollutants to the Arctic in a large suite of models, allowing us to characterize the relative importance of emissions from different source regions as well as uncertainties in current understanding. As it is difficult to determine the source regions for Arctic pollutants directly from observations, and there have been some apparent inconsistencies in previous modeling studies (Law and Stohl, 2007), we believe that examining results from a large suite of models is a useful endeavor.

2 Description of simulations and analyses

A series of simulations were designed to explore source-receptor relationships (i.e. the contribution of emissions from one region, the source, to concentrations or deposition in a receptor region). The source regions were chosen to encompass the bulk of Northern Hemisphere emissions: Europe (EU: 10W-50 E, 25N-65N, which also includes North

Africa), North America (NA: 125W-60W, 15N-55N), East Asia (EA: 95E-160 E, 15N-50N) and South Asia (SA: 50E-95E, 5N-35N) (Figure 1). Northern Asia (Russia) was not included as a source region as its total emissions of most pollutants are comparatively small (at least for anthropogenic sources). However, given their proximity to the Arctic, emissions from this area can contribute substantially to Arctic pollution and so we caution that our analyses are not exhaustive. We define the Arctic poleward of 68 N as our receptor region. A base case simulation was initially performed using each model's own present-day emissions. Additional simulations then explored the response to a 20% reduction of anthropogenic emissions of nitrogen oxides (NO_x) alone, carbon monoxide (CO) alone, or all anthropogenic ozone and aerosol precursors except methane from each of the four source regions. Participating models are listed in Table 1. We analyze the response of Arctic concentrations of trace gases and aerosols and deposition of BC in both Greenland and elsewhere in the Arctic.

As models used different base case anthropogenic emissions, the 20% perturbations differed in absolute amounts. Hence we generally analyze changes in Arctic abundances normalized by the regional emissions change between the control and the perturbation using direct emissions (CO, BC) or the dominant precursor (sulfur dioxide (SO_2) for sulfate (SO_4), NO_x for ozone (O_3)). Hereafter we refer to this quantity, in mixing ratio per Tg emission per season or year, as the Arctic sensitivity to source region emissions. With the exception of non-linearities in the response, this separates out the effect of intermodel differences in emissions. Uncertainties in emissions are of a different character than the physical uncertainties that we also explore, as the former depend on the inventories used to drive models while the latter are intrinsic to the models themselves.

The response to emissions changes in all four HTAP source regions were analyzed. All these simulations included a minimum of 6 months integration prior to analysis to allow for stabilization, followed by a year of integration with 2001 meteorology (2001 was chosen to facilitate planned comparisons with campaign data for that year). Differences in meteorology were present, however, as models were driven by data from several reanalysis centers, or in some cases meteorology was internally-generated based on prescribed 2001 ocean surface conditions. Additionally, some models directly prescribed meteorology while others used linear relaxation towards meteorological fields. Note that

the North Atlantic Oscillation index was weakly negative during 2001, while the broader Arctic Oscillation index showed a stronger negative value during winter, with weak positive values for most of the remainder of the year. These indicies are reflective of the strength of the Northern Hemisphere westerly winds, with weaker winds associated with reduced transport to the Arctic (Eckhardt et al., 2003; Duncan and Bey, 2004; Sharma et al., 2006).

Idealized tracer simulations were also performed to isolate the effects of intermodel differences in transport from other factors affecting trace species distributions. For these simulations, all models used identical emissions of a CO-like tracer with a prescribed globally uniform lifetime of 50 days. A second tracer ("soluble CO") used the same emissions and lifetime, but was subjected to wet deposition as applied to sulfate. Three additional tracers used identical anthropogenic volatile organic compound (VOC) emissions and had prescribed lifetimes of 5.6, 13 and 64 days. The range of model results in these simulations (other than the soluble tracer) thus reflects only the variation in the transport algorithms used and in the meteorology used to drive the transport (which differed among models as discussed above). Emissions from different source regions were tagged for the CO-like and soluble CO tracers (but not for the VOC-like tracers). We examine the Arctic concentration of the regionally tagged tracer divided by the source region emission, analogous to the Arctic sensitivity described above (though these are absolute concentrations in a single run rather than a difference between a control and a perturbation run).

All results for the Arctic are based on area-weighted averages. Results for Greenland are averaged over the entire Greenland land area, including the area south of that defined here as Arctic, neglecting model grid boxes near the coast that contain more ocean than land area. Surface values are those in the lowest model layer. The global mean pressure of this layer varies from 939 to 998 hPa across models (though different representations of topography could lead to larger variations at some points), suggesting that for most locations differences in definition of the surfacew layer will contribute only minimally to intermodel variations. Values at 500 and 250 hPa levels are interpolated from model output. All seasons refer to their boreal timing.

Figure 1. The Arctic and the four source regions (shaded) used in this study.

3 Modeled sensitivities, concentrations and deposition

In this section, we first consider Arctic sensitivities and concentrations in the idealized simulations using the passive tracer with a prescribed 50 day lifetime for which regional emissions were tagged (section 3.1). We then analyze similar quantities for both gases and aerosols in the simulations using realistic chemistry and physics (section 3.2). Finally, we investigate model results for the deposition of black carbon to the Arctic (section 3.3).

3.1 Prescribed lifetime tracer

Transport of European emissions to the Arctic surface is clearly largest in winter (Figure 2) based on results for the CO-like 50-day lifetime tracer from 8 models (Table 1). During all seasons, the Arctic surface level is most sensitive to European emissions (Figure 2). In the middle troposphere, the sensitivities to emissions from Europe and North America are usually comparable, sensitivities to East Asian emissions are somewhat less, and sensitivities to South Asian emissions are quite small outside of summer (probably because of the greater distance to the Arctic from this region (Figure 1)). These results are consistent with the 'polar dome' or 'polar front' that impedes low-

level transport from relatively warm and humid areas such as North America and East Asia into the Arctic during the cold months while allowing such transport at higher altitudes from those regions and at low-levels from Eurasia, which often lies within the polar dome (Law and Stohl, 2007; Klonecki et al., 2003; Stohl, 2006). During summer, when the polar front is at its furthest north, emissions from all four source regions have a comparable influence on the Arctic surface (per unit emission), with a slightly larger contribution from Europe.

In the upper troposphere, the models tend to show comparable sensitivities for all four regions. The spread of model results is typically similar to that seen at lower levels. Sensitivities in the upper troposphere are greatest in summer for all regions, consistent with the surface for Asian emissions but opposite to the surface seasonality seen for European emissions. The largest sensitivities in the upper troposphere are to summertime Asian emissions.

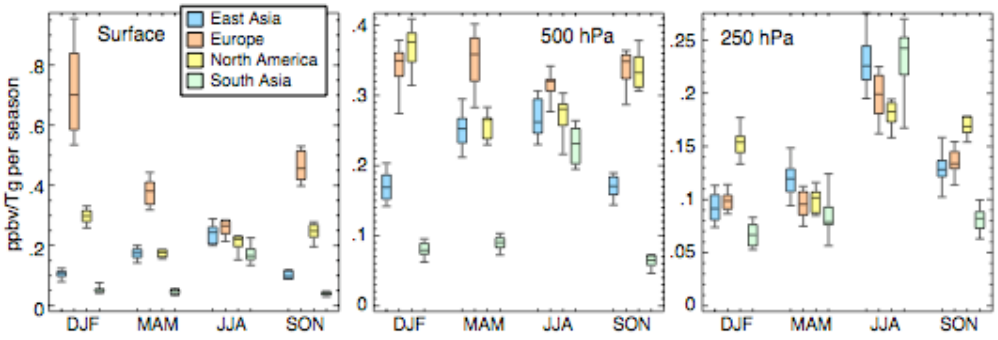

Figure 2. Arctic sensitivity at three levels for the seasonal average CO-like tracer in terms of mixing ratio per unit emission from the given source region in the prescribed 50-day lifetime tracer simulations (8 models). Boxes show the central 50% of results with the median indicated by the horizontal line within the box, while the bars indicate the full range of model sensitivities.

3.2 Active gas and aerosol species

We now investigate the more realistic, but more complex, full gas and aerosol chemistry simulations. We sample only the models that performed the perturbation runs for a particular species (Table 1). The divergence in model results in the control run is extremely large in the Arctic. For example, annual mean CO varies by roughly a factor of 2-3 at all levels examined. Arctic sulfate varies across models by factors of 8 at the surface, 600 in the mid-troposphere, and 3000 in the upper troposphere. Though some models clearly must have unrealistic simulations, we purposefully do not exclude any models at this stage as our analysis attempts to identify the sources of this enormous divergence among models. We note that the diversity of model results in the Arctic is not terribly different from that seen elsewhere. Examining annual means using equally sized areas over the US and the tropical Pacific, polluted and remote regions, respectively, we find CO variations of roughly a factor of 2 across models, and standard deviations at various altitudes are 14-22% of the mean in those regions, only slightly less than the 22-29% in the Arctic. For sulfate, the range and standard deviation across models are smaller at the surface for the US, where they are a factor of 6 and 36% (versus Arctic values of a factor of 8 and 52%), but greater for the remote Pacific, where they are a factor of 40 and 62%. At higher levels, the range is only slightly less than that seen in the Arctic, and standard deviations are 86-124% of the mean in the other regions, also similar to the 98-99% seen in the Arctic.

We first examine the total contribution from each source region to the annual average gas or aerosol amount in the Arctic. This includes the influence of variations in emission inventories among the models (Table 2). These variations are quite large, often as great as a factor of two between minimum and maximum. The range of SO_2 and BC emissions used in the models is especially large for Europe compared to other regions, probably because of rapid changes with time and the many estimates that have been made for European emissions. For the multimodel mean, we find that at the surface, European emissions dominate the Arctic abundance of sulfate and BC, and to a lesser extent CO (Table 3 and Figure 3). Arctic surface ozone responds most strongly to NO_x emissions from North America, with substantial responses to emissions from Europe and East Asia as well. In the mid-troposphere, sulfate abundances are again dominated by European

emissions, but the contribution from East Asia is almost as large as that from Europe for BC. By the upper troposphere, both total sulfate and BC show the largest impact from East Asian emissions, especially for BC (Figure 3). The amount of CO from each region also undergoes a shift with altitude, as European emissions become steadily less important relative to East Asian and North American emissions. The relative importance of regional NO_x emission changes to Arctic ozone is less dependent upon altitude, with the largest contribution from North America at all levels. The results are consistent looking at either the multi-model mean or median values. These are generally quite similar for CO and ozone, while the median is typically lower than the mean for the aerosols, but the relative importance of different regions is almost unchanged between these two statistics (Table 3).

We next turn to Arctic sensitivities (Arctic concentration change per unit source region emission change, hence removing the influence of emission inventory variations across models) rather than total Arctic concentrations, first examining seasonal sensitivities for CO, SO_4, and BC (Figure 4). The median Arctic surface sensitivities for all three species are greatest for European emissions, by roughly a factor of ~3-6 compared with the sensitivities to emissions from other regions. Median sensitivities in the mid-troposphere are again largest for European emissions in nearly all cases, by a few percent to a factor of two. In the upper troposphere, median sensitivities are comparable for East Asian, European and North American emissions. In many cases, sensitivities to South Asian emissions are substantially less than those for other regions. This is not the case for aerosols during winter and spring though, when sensitivities to South Asian emissions are large and sometimes greater than those for any other region. However, the range of sensitivities among models is quite large, especially for the aerosols.

Examining the CO sensitivity to the emissions with the greatest impact (EU, NA and EA), the range of annual average values is roughly a factor of 2-3 among the 11 models. The standard deviation is much smaller (~20-30%), indicating that most models are relatively consistent. The seasonality of the Arctic CO sensitivity depends on the source region. At the surface, the multimodel mean sensitivity to European emissions clearly maximizes in winter, while for North American and especially East Asian emissions the maximum sensitivity is in spring. These two regions also differ in their seasonality,

however, with the minimum sensitivity in fall for East Asian emissions but in summer for North American emissions.

For surface sulfate, Arctic sensitivities in individual models vary greatly. For the annual average, the range spans 2.8 to 17.4 pptm/(Tg S)/season. (Note that the annual average values are in units of pptm/Tg/season for comparison with seasonal sensitivities. Values in pptm/Tg/year are ¼ of these season numbers). Interestingly, the models separate into two groups: of the 13 models, 6 have annual average sensitivities below 4 pptm/(Tg S)/season, while the other 7 have sensitivities of 7.2-17.4 pptm/(Tg S)/season. Seasonal surface sensitivities show an even larger spread (Figure 4). Median sensitivities to European emissions are comparable in all seasons though the spread in the central 50% of models is greatest in winter and spring. Sulfate sensitivities to East Asian and North American emissions maximize in spring, as for CO. In the mid-troposphere, sensitivities are generally largest for European emissions, while in the upper troposphere they are greatest for South Asian emissions in spring and East Asian emissions during other seasons.

BC sensitivities show spring maxima for surface responses to East Asian and North American emissions, as for sulfate and CO. For European emissions, however, BC sensitivity shows a strong winter maximum and a fall sensitivity that is also enhanced over the spring and summer values. The mean winter sensitivity to European emissions of 30 pptm/(Tg C)/season is much larger than the sensitivities to European emissions during the other seasons (means of 9-17 pptm/(Tg C)/season). The enhanced winter sensitivity results from both faster transport during winter and slower removal at this time as the Arctic is stable and dry (Law and Stohl, 2007). During spring, summer and fall, the mid-troposphere, like the surface, is most sensitive to European BC emissions. During winter, however, sensitivity to North American and European emissions is almost identical. Interestingly, the seasonality of sensitivity can vary with altitude: the sensitivity of surface BC to European emissions is greatest in winter, while the sensitivity of mid-tropospheric BC to European emissions maximizes in summer (sulfate sensitivities show fairly similar behavior). The sensitivity to North American and East Asian emissions maximizes in spring. Sensitivities in the upper troposphere maximize in summer for East Asia, Europe and North America. Though the multimodel mean surface and mid-

tropospheric sensitivities are clearly greatest for European emissions, the annual average BC sensitivity to European emissions varies greatly among models: from 0.6 to 12.8 pptm/(Tg C)/year for the surface and from 0.1 to 14.9 pptm/(Tg C)/year at 500 hPa.

The sensitivity of Arctic surface ozone to source region NO_x emissions is quite different than that for the other species examined here (Figure 4). Note that MOZECH and UM-CAM were excluded from the O_3/NO_x analysis due to imbalances in their nitrogen budget diagnostics. Sensitivity to winter European emissions is negative for most models (i.e. reduced NO_x emissions leads to more Arctic ozone). This results from direct reaction of NO_x with ozone in the relatively dark conditions that much of the high-latitude European emissions encounter. The cancellation of negative winter and positive non-winter ozone sensitivities leads to a lower annual average European influence on Arctic surface ozone than for other species (Table 3). Spring surface ozone concentrations show comparable sensitivities to East Asian, European and North American emissions, while summer concentrations are most sensitive to European and fall to European and North American emissions. During winter, sensitivities to South Asian emissions are nearly as large as those for East Asian and North American emissions. Sensitivities in the mid-troposphere show a similar pattern to those seen at the surface (Figure 4). The upper troposphere shows comparable sensitivities for all four of the source regions, with greatest sensitivity to South Asian emissions in winter and spring, though North American emissions have the largest annual average influence (Figure 3).

The magnitude of the sensitivity increases with altitude for SO_4 and O_3, stays roughly constant for BC, and decreases for CO. This may reflect the greater removal of soluble aerosols and ozone precursors at low levels relative to insoluble CO. In addition, both SO_4 and O_3 are produced photochemically at higher altitudes, while CO is photochemically removed aloft.

A critical result of the analysis is that for both sensitivities and totals, discrepancies between models are systematic, so that the relative importance of different regions is robust despite the large differences among models in the magnitude of the contribution from a particular region. For example, every participating model finds the largest total contribution to annual average surface SO_4, BC, and CO to be from Europe. Similarly, all

models find that in the upper troposphere, East Asia is the largest annually-averaged source for BC, with all but 3 giving first rank to East Asia for sulfate and CO as well. Looking at annual totals, 9 out of 11 models have a larger contribution to 500 hPa Arctic ozone from North America than from Europe even though the standard deviations overlap substantially (Table 3). Every model finds that the Arctic sensitivity during winter, fall and spring for surface SO_4, BC and CO is largest for European emissions. This holds even during summer for sulfate and BC, while for CO all but 1 model have the greatest sensitivity to European emissions.

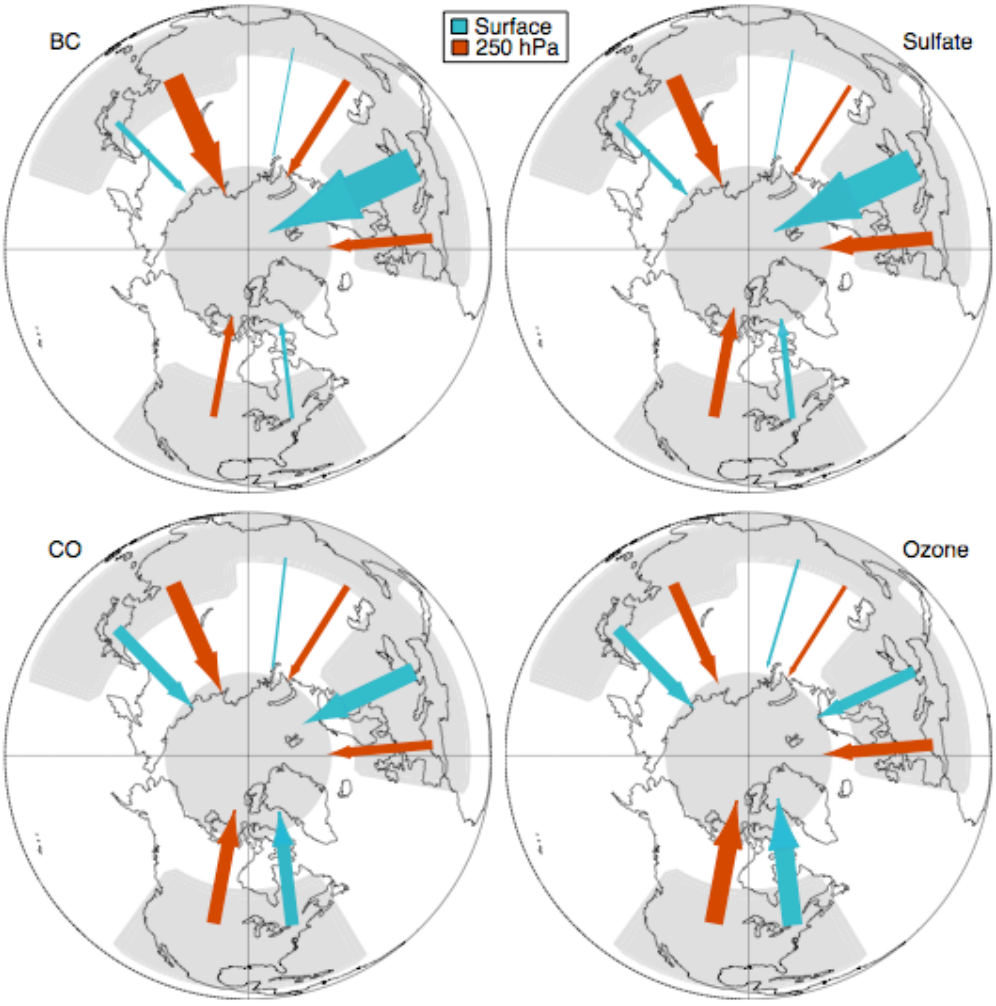

Figure 3. Relative importance of different regions to annual mean Arctic concentration at the surface and in the upper troposphere (250 hPa) for the indicated species. Values are calculated from simulations of the response to 20% reduction in anthropogenic emissions of precursors from each region (using NO_x for ozone). Arrow width is proportional to the

multimodel mean percentage contribution from each region to the total from these four source regions (as in Table 3).

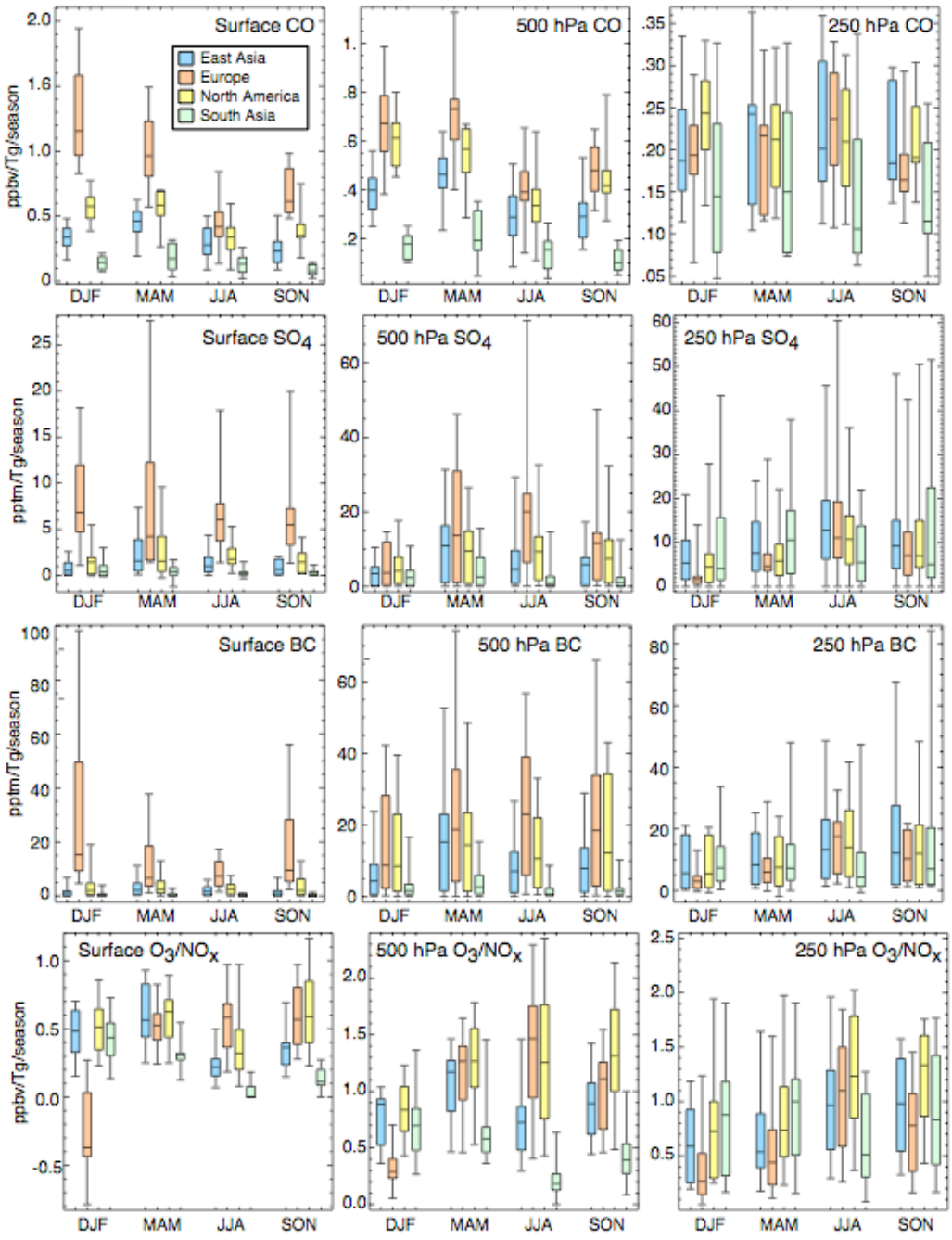

Figure 4. Arctic sensitivity to emissions from the given region for seasonal averages of CO, sulfate, BC and ozone mixing ratios at the indicated heights. Sensitivities are the difference between the simulation perturbing a given emission and the control, normalized by the emissions change in the species (CO, BC) or its primary precursor (S in SO_2 for SO_4, N in NO_x for O_3) in the indicated source region. Symbols as in Figure 2. Note change in vertical scale between columns.

3.3 Arctic deposition of black carbon

In addition to atmospheric concentrations, deposition of BC to the Arctic is of particular interest due to its climate impact, as discussed previously. We now explore the relative importance of the various source regions to BC deposition to Greenland and to the rest of the Arctic, and use the multimodel results to characterize the robustness of these results. We examine both the total BC deposited and also the BC deposition sensitivity by calculating the Tg deposited per unit area per Tg source region emission. Deposition is calculated on all surfaces, including open ocean, though albedo will be affected by the flux to snow and ice surfaces.

Deposition of BC to the Arctic (excluding Greenland) is most sensitive to emissions from Europe in every season (Figure 5), and is generally quite similar to the BC surface mixing ratio sensitivity (section 3.2). That sensitivity to European emissions is greatest is clear even though the spread in model sensitivities is very large, more than an order of magnitude in most seasons for European emissions, for example. The large range often results from just one or two models. For example, the deposition sensitivities for the Arctic (except Greenland) during summer for European emissions are within 0.04 to 0.32 m^{-2} 10^{-11} in 8 models, while the remaining two have values of 0.76 and 2.14 m^{-2} 10^{-11} (ECHAM5-HAMMOZ is excluded from the BC deposition analyses owing to apparent problems in their deposition diagnostics). However, even the range within the central 50% of models is substantial in other seasons (Figure 5). Median sensitivities are largest in fall and winter for European emissions, but in spring, summer and fall for North American emissions and in spring for East Asian emissions. Examining the BC deposited per unit BC emitted (i.e. multiplying the values in Figure 5 by area), the multi-model mean percentage of emissions that are deposited in the entire Arctic (including Greenland) is 0.1% for South Asian, 0.5% for East Asian, 1.0% for North American and 3.6% for European emissions.

Deposition of BC to Greenland shows different sensitivities compared with the rest of the Arctic, with the largest response to North American emissions in non-winter seasons (Figure 5). This results from the high topography of Greenland, which allows the inflow

of air from the relatively warm and moist North American, and to a lesser extent East Asian, source areas to occur more easily there than in the rest of the Arctic (Stohl, 2006).

Examining the total BC deposition response to 20% regional emissions changes, we find similar results for the Arctic excluding Greenland as for the sensitivity (compare Figures 6 and 5). Most significantly, total deposition is greatest from Europe in every season. Again the spread of results is large, but the central 50% of models are distinctly separated for Europe from other regions in all seasons but spring. In that season, East Asian emissions take on greater importance as they are large and the sensitivity to East Asian emissions maximizes in spring (Figure 5). For the annual average, total deposition to the Arctic outside of Greenland is clearly dominated by European emissions (Table 4). We reiterate that emissions from Northern Asia (Russia) were not studied in these analyses.

The change in total deposition to Greenland in response to 20% regional emissions changes is roughly evenly split between the impact of European and North American emissions (Figure 6). Deposition of BC from East Asia is as large or nearly as large as that from these regions in spring and summer, though not in other seasons or in the annual average. The spread of results for total deposition to Greenland is substantially larger for totals than for sensitivities for East Asia and Europe, reflecting the large variation between models in emissions from or within these regions. Looking at the annual average total deposition to Greenland, it appears at first that the uncertainties are too large to allow determination of the relative importance of emissions from the various source regions (Table 4). However, the distribution of results is neither normally distributed nor random. To test the impact of 'outlier' models, we calculated deposition statistics leaving out the models with the lowest and highest deposition rates (Table 4). The model with the largest deposition contributes a large fraction of the standard deviation. The lowest does not, however, as the distribution of results is highly skewed towards values considerably above the mean. To test for systematic effects across regions, we also examined the relative importance of each region across models. While one standard deviation of the deposition values for a given region nearly always encompasses the values for the other regions, in fact the model-to-model differences are systematic. Nine of the 10 models have the identical order: greatest deposition to Greenland from North American emissions, followed by European, East Asian and lastly

South Asian emissions. Deposition to the Arctic (exclusive of Greenland) is similarly skewed (Table 4) and robust in the regional rankings across models. Hence as for atmospheric mixing ratios and concentration sensitivities (section 3.2), the relative contribution of emissions from the various source regions to BC deposition can be determined with much higher confidence than the magnitude for any particular region.

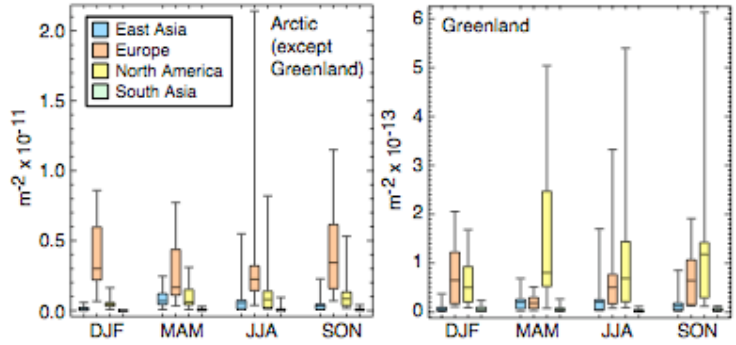

Figure 5. Sensitivity of Arctic-wide (left, excluding Greenland) and Greenland (right) BC deposition to regional emissions (Tg deposition per Tg emission per unit area per season). Values are calculated from the 20% anthropogenic emissions perturbation simulations.

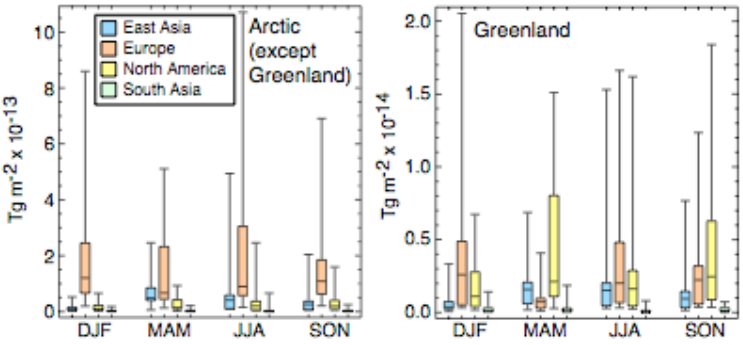

Figure 6. Total Arctic-wide (left, excluding Greenland) and Greenland (right) BC deposition (Tg deposition per unit area per season) in response to 20% anthropogenic emission change from each source region.

4 Comparison with Arctic observations

Observational datasets are quite limited in the Arctic, making it challenging to reliably evaluate models in this region. Nevertheless, it is worth investigating how well the

models perform and how our results are influenced by any models which appear to be clearly unrealistic in their Arctic simulations. In this section, we compare the modeled and measured seasonal cycles of surface CO, ozone, sulfate and BC for selected stations in the Arctic. Root-mean-square (RMS) errors between the monthly mean modeled and observed values are used to evaluate the models, though this is clearly only one possible measure of model/observation agreement. We then evaluate the influence of screening out less realistic models in section 5.

The models exhibit a large spread for CO at Barrow and Alert (Figure 7), though most have a fairly reasonable seasonal cycle based on comparisons with observations (Novelli et al., 1998). Many of the models do a good job of reproducing summer and fall CO amounts, but nearly all underestimate the late winter-early spring maximum (as in previous studies, e.g. (Shindell et al., 2006)). All models have average RMS errors for the two sites of between 17 and 40 ppbv, with the exception of two that have RMS values of 54 and 83 ppbv. We note that no model stands out as substantially better than the others (the model with the second lowest RMS error has a value only 3 ppbv greater than the lowest score). While the EMEP model stands out from the others with clearly larger values during fall (Figure 7), it is not obviously better or worse in comparison with observations over the full annual cycle. Note also that none of the outlying models (those labeled in Figure 7) has CO emissions distinctly different from the other models. For example, the two models with greatest RMS errors have global CO emissions of 1115 Tg/yr and European emissions of 74 and 111 Tg/yr, both well within the range across all models of 1018-1225 Tg/yr for global and 70-130 Tg/yr for European emissions. Hence excluding the two models with highest RMS error provides a reasonable subset for repeating the CO analyses.

Comparison of ozone observations (based on updates from (Oltmans and Levy, 1994)) with the models shows that the simulations again have a fairly wide spread. Modeled values are generally reasonable during summer and fall at Barrow, though some models have underestimates, but agreement is poor during winter and spring. Nearly all models underpredict ozone at Summit. Those that overestimate ozone at Barrow during spring often do a better job at Summit, as they fail to capture the large observed springtime contrast between these two sites. This leads to comparable error scores to other models.

All models have average RMS errors of 7-12 ppbv except for STOCHEM-HadGEM1 with a value of 21 ppbv. We find that exclusion of a single model, however, does not appreciably change the results presented previously.

For sulfate observations, we use data from the EMEP network's station on Spitsbergen (Hjellbrekke and Fjæraa, 2007) and data from Alert (Sirois and Barrie, 1999), though the Alert data covers earlier years. The sea-salt component has been removed from these data. The models generally perform poorly in simulating Arctic sulfate (Figure 7). Most substantially underestimate Arctic concentrations, by more than an order of magnitude in several models. Many that show annual mean sulfate concentrations of about the right magnitude have seasonal cycles that peak in summer or fall, while the observations show a spring maximum. This leads to RMS error values that are fairly large for all models, with multi-model means of 201 (Alert) and 272 (Spitsbergen) pptm. However, models cluster in two groups, with none having average values for the two sites between 190 and 250. Hence we can test if the subset of models with RMS values below 190 pptm yields a different result than the full suite of models.

Note that comparison with measurements taken from 1996-1999 at Denali National Park (from the Interagency Monitoring of Protected Visual Environments: IMPROVE, http://vista.cira.colostate.edu/improve) at 64°N (just outside the Arctic region we use here) show similar discrepancies between models and observations. The multi-model mean RMS error at Denali is 249 pptm. Hence although the comparison at Alert may be influenced by differing emissions during the 1980s, the overall results suggest that discrepancies between models and observations occur throughout the high latitudes. As for CO, there is no clear relationship between the emissions used by the models and their Arctic simulations. For example, SO_2 emissions from Europe, which have the largest influence on the Arctic, are 15-20 Tg S/yr (mean 18 Tg S/yr) in the group of models with lower RMS values, and 8-25 Tg S/yr (mean 16 Tg S/yr) in the high RMS group, of which half the models have emissions within the range seen in the lower RMS group. Given that models also show large diversities over the US, where emissions are relatively well-known, and since the model-to-model sulfate concentrations vary much more than the model-to-model emissions, we believe the cause of the model/measurement discrepancies

is largely different representations of aerosol chemical and physical processing and removal rather than emissions (see Section 5.2).

We also attempted to evaluate the simulation of BC in the models. Comparison with observations from Sharma et al (2006) suggests that models greatly underpredict BC in the Arctic (Figure 7). However, the available measurements are in fact equivalent BC (EBC), which is obtained by converting light absorbed by particles accumulated on a filter in a ground-based instrument to BC concentrations. Uncertainties in the optical properties of BC make this conversion quite challenging. Additionally, other light absorbing species such as OC and especially dust influence the measurements, so the EBC would tend to be high relative to actual BC. This is consistent with the sign of the model/observations difference (Figure 7), though the other species are expected to have fairly small contributions in the Arctic, and hence a substantial underestimate of BC in the models is likely. Models also appear to substantially underestimate BC in comparison with IMPROVE data from Barrow (updated from (Bodhaine, 1995)), which itself differs significantly from the Sharma et al (2006) data. The Barrow data is also derived from optical absorption measurements. Given the large apparent discrepancies for BC for all models, we conclude that it is not feasible to determine the relative realism of the models using currently available data, though it appears that models with a greater transport of BC to the Arctic are in general more realistic.

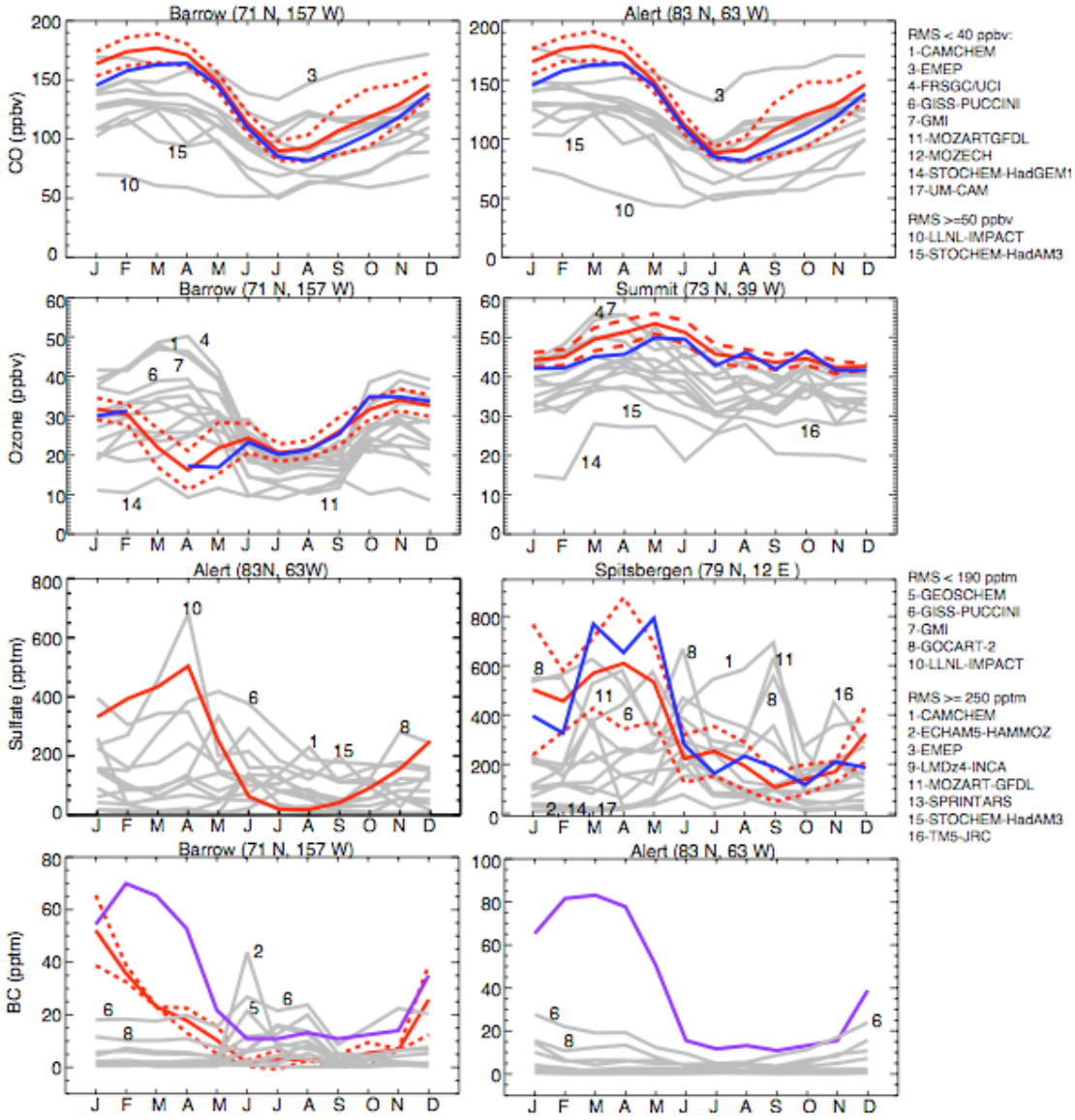

Figure 7. Observed and modeled seasonal cycles of trace species surface concentrations at the indicated Arctic sites. Model results in all panels are in grey. Plots for CO (top row) and ozone (second row) show observations from the NOAA Global Monitoring Division, with 1992-2006 means and standard deviations in red (except for Summit O_3, which is 2000-2006) and 2001 in blue. Sulfate plots (third row) show observations from Alert during 1980-1995 (left) and from the EMEP site in Spitsbergen during 1999-2005 in red, with 2001 Spitsbergen data in blue. BC data (bottom row) are from the IMPROVE site at Barrow during 1996-1998 (red), and from Sharma et al (2006) for both Barrow and Alert using equivalent BC over 1989-2003 (purple). Models are listed by RMS error

scores to the right of each row using the groupings discussed in the text. Models that are separated from others are labeled with the numbers as in the text at right (or Table 1).

5 Causes of intermodel variations

In this section, we investigate the role of model-to-model differences in transport, photochemistry and deposition, and emissions in creating the diversity of results seen in the Arctic. This is accomplished by comparison of the prescribed lifetime simulations with the full chemistry and physics simulations and by examining the correlation between Arctic concentrations and diagnostics such as residence times.

5.1 Isolating processes governing variations in CO and ozone

We first compare the intermodel variability in Arctic sensitivities in the run with the prescribed lifetime "CO-like" tracer to that with realistic CO. As the two sets of experiments do not use directly comparable CO, we analyze the standard deviation as a percentage of the mean response (the fractional variation) among models. All models in the analysis performed both the prescribed lifetime and full chemistry runs.

The fractional variation of sensitivity is always larger in the full chemistry analyses than in the prescribed 50 day lifetime case (numerical values in Figure 8). The relative size of the fractional variations in the prescribed lifetime and full chemistry runs depends on the altitude analyzed and the source region. At the Arctic surface, the intermodel fractional variation in the prescribed lifetime runs is 9-14%, roughly two-thirds that seen in the full chemistry runs (16-26%) for all regions (Figure 8). This indicates that differences in modeled transport to the Arctic play an important role in CO near the surface. In the middle troposphere, transport and chemical oxidation by OH contribute a comparable amount to intermodel differences in Arctic CO, while in the upper troposphere transport plays a much smaller role. At the surface and in the mid-troposphere, adding in the intermodel variation in emissions (i.e. no longer normalizing by emissions) leads to larger fractional variances across the models. This is especially so for East Asia, where including the intermodel variation in emissions nearly triples the fractional variance of

the Arctic response at the surface and middle troposphere across models. The effects are smaller for emissions from Europe or North America at these levels, where emissions variations add ~5-13% to the fractional variance, a comparable range to that from transport (8-14%) and oxidation (6-11%) variations among models. Emissions uncertainties from South Asia have an even smaller impact than those from Europe or North America, barely changing the fractional variance.

Thus the intermodel variation in the influence of source region CO emissions on the Arctic surface and mid-troposphere is dominated by emissions for East Asia, by transport and oxidation for South Asia, and all three terms (transport, oxidation and emissions) play comparable roles for Europe and North America. In the upper troposphere, the intermodel fractional variations are dominated by oxidation differences, whose importance gradually increases with altitude. We note, however, that while the 250 hPa intermodel differences are important, the variation across the central 50% of models in CO sensitivity in the upper troposphere is only ~40%, among the smallest range for any species at any level (Figure 4).

We now investigate the dependence of the results on the quality of the model's Arctic CO simulation. Including all models, the fractional variation is 20-26% for surface and mid-troposphere sensitivities to European, East Asian and North American emissions, and is 31-35% for South Asian emissions. Using only the subset of models showing better agreement with observations (9 of 11 models), it decreases to 11-13% for surface and mid-troposphere sensitivities to East Asian and North American CO emissions, 16% and 22% for surface and mid-troposphere sensitivities to European emission, respectively, and 23-25% for South Asian emissions. There is no appreciable difference between using all models or restricting the analysis to the subset when calculating the standard deviations in the upper troposphere. In either case these are 24-29% for European, East Asian and North American emissions. The sensitivity to South Asian CO emissions in the upper troposphere shows a very large standard deviation across models (45-47%), perhaps related to variations in model simulations of tropical convective transport. However, its contribution per unit emission is relatively small. Hence screening models by their ability to match observations can substantially reduce the intermodel variations even though in this case only 2 models were removed. We conclude that the Arctic-wide

response to source region emissions perturbations can be simulated relatively reliably for a long-lived species such as CO. This is especially true for quality-screened models, in which case fractional variations in the mid and lower troposphere are 22% or less for CO sensitivity to emissions from Europe, and 13% or less for emissions from East Asia or North America.

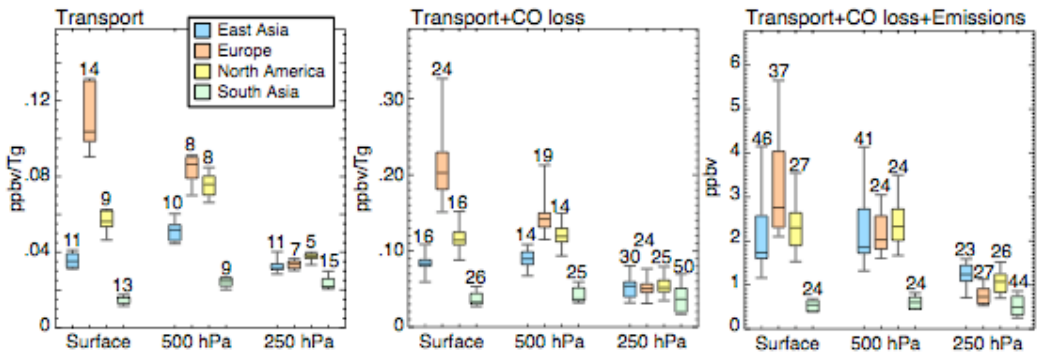

Figure 8. Annual Arctic average carbon monoxide response to source region emissions as a function of processes included in the models. The influence of transport is shown via the Arctic sensitivity in the prescribed 50 day lifetime CO-like tracer runs (left). The influence of transport plus CO oxidation is given by the sensitivity in the full chemistry run (center). The influence of transport plus oxidation plus emissions is also given by the full chemistry run, this time without normalization by the source region emissions change (right). Numerical values over each bar give the fractional variation (standard deviation as a percentage of the mean). Symbols as in Figure 2.

Though model results are relatively consistent for CO, it is interesting to examine the relationship across models between the Arctic sensitivities and the global mean chemical lifetime (lifetimes for portions of the globe could not be calculated using the available diagnostics). A high correlation would indicate that the removal rates of CO (by oxidation) play an important role in intermodel variations in sensitivity. We find that either using all models or the quality-screened subset there is little correlation between CO sensitivity and global mean lifetime for the surface and mid-troposphere, except for South Asian emissions (Table 5). There is some correlation for all regions in the upper troposphere (R^2 0.4-0.7). Hence it appears that the CO chemical lifetime, a measure of

the CO oxidation rate, does not play a large role in determining the sensitivity of the Arctic to NA, EU and EA emissions perturbations below the upper troposphere. These results are consistent with the increasing importance with height of oxidation seen in the comparison between the prescribed lifetime and full chemistry simulations. For emissions from South Asia, which have to travel further to the Arctic, the chemical lifetime does appear to play an important role, especially in the mid and upper troposphere.

Ozone's response to NO_x emissions perturbations can be of either sign, indicating non-linearities in chemistry that preclude explanation via linear correlation analysis between the response and ozone's lifetime. We can, however examine correlations between Arctic ozone sensitivity and intermodel variations in ozone dry deposition or transport (using the passive tracer simulations for the latter). We find that model-to-model variations in dry deposition account for little of the spread in Arctic ozone sensitivity to NO_x perturbations, even at the surface (R^2<0.3 at all levels, <0.1 at surface). Correlations between Arctic ozone sensitivity and transport (using the prescribed lifetime tracer values. as in the left panel of Figure 8, for each model) are similarly weak at the surface and 250 hPa (R^2<0.25). In the mid-troposphere (500 hPa), however, correlations are R^2=0.4 to 0.5 for NA, EA and SA, indicating that at those levels transport variations account for roughly half the intermodel variation in Arctic ozone sensitivity. At other levels, however, it appears that model-to-model differences in the non-linear ozone photochemistry must play the dominant role in the intermodel spread of sensitivities. Consistent with this, annual mean ozone sensitivity to NO_x perturbations shows a variation across models of 35-80% of the mean across regions and altitudes, which is substantially larger than the 8-15% in the prescribed 50 day lifetime tracer experiments

5.2 Isolating processes governing variations in aerosols

We examine the relationship between the Arctic concentrations and the aerosol lifetimes, as for CO. For aerosols, however, we are able to calculate the global residence time for regional emissions perturbations. These are determined from the change in burden over the change in removal rates in the regional perturbation experiments. Note that this calculation implicitly assumes that the residence time is the same in the two experiments,

which given the relatively small emissions perturbations imposed in our experiments should be a good approximation.

We also compare with the prescribed lifetime tracer results to estimate the relative importance of transport variations among models to the total range in results. The prescribed 5.6 and 13 day lifetime anthropogenic VOC-like tracers have lifetimes most comparable to those of aerosols. Comparison of the different lifetime VOC tracers shows that the spread of model results is inversely related to lifetime (Table 6), as might be expected. The relationship is not linear, however, and depends on altitude as well as lifetime. Additionally, the solubility of some aerosols links them to the hydrologic cycle much more closely than for these tracers, so the comparison with the prescribed lifetime VOC or insoluble CO tracer results isolates the influence of dry transport (i.e. excluding transport of species in the aqueous phase). The role of transport that can be identified from the prescribed lifetime tracer simulations also does not include linkages between transport and wet removal that result from removal rates varying with location, such as for wet removal processes that depend on local precipitation. Hence transport has a specific, limited meaning in our analysis.

The range of intermodel variations in Arctic sensitivity is much larger for BC than for CO (Figure 4). The intermodel variation in residence time for BC among models is roughly a factor of 2 and accounts for most of the spread (Table 5). This variation is much greater than the variation in efficiency of dry transport to the Arctic at most levels from any region as seen in the prescribed lifetime simulations (e.g. Figure 8), even accounting for the intermodel transport variations being roughly twice as large for a tracer with BC's lifetime than with CO's (Table 6). Hence the other factors affecting residence time, including aerosol aging from hydrophobic to hydrophilic and rainout/washout of the aerosols, appear to play important roles in governing the Arctic sensitivity to regional BC emissions from middle to higher Northern latitudes (EU, NA, and EA). In other words, the large variations in how long BC remains in the global atmosphere seems to be more important in determining how much reaches the Arctic than are dry transport differences or local Arctic removal processes (which contribute only a minor fraction of the global removal). This result is consistent with the strong sensitivity in the export efficiency of Asian BC to the conversion lifetime from hydrophobic to

hydrophilic seen in a study based on 2001 aircraft data (Park et al., 2005). For emissions from South Asia, the global annual mean residence time of BC is less closely correlated with the Arctic sensitivity. Hence for emissions from this region, both intermodel variations in BC residence times and in transport appear to be important factors in creating model diversity.

For sulfate, the fractional variation in annual average sensitivity to regional emissions across models is ~68-112%, much greater than that seen in the prescribed 50 day lifetime runs where fractional variations were only ~8-15% (Figure 8), or the 6-20% variations in the response to global emissions for the 5.6 day lifetime tracer (Table 6) (note that the intermodel variations in reponse to global emissions are 0-50% less than those for regional emissions in the 50 day lifetime experiments). This suggests that for sulfate, variations in large-scale physical and chemical processing of aerosol (removal of sulfate and/or SO_2, oxidation of SO_2, etc) account for a major portion of the divergence between models. This is consistent with the order of magnitude increase in model-to-model variations going from insoluble to soluble passive tracers that are otherwise identical (Table 6). When intermodel emissions variations are not removed from the sulfate response calculations, the annual average fractional variance increases only modestly (~10%), to 79-120% across the models. Thus emissions differences appear to play a minor role in the model-to-model variations.

Sulfate's global mean residence time in the models ranges from 2.7 to 11.2 days. Aside from the two models with these values, the other 12 all have lifetimes between 3.2 and 7.4 days. Hence the spread in global residence times is small compared with the spread in Arctic sensitivities (Figure 4). Correlations between these two quantities are fairly weak at the surface, but more significant aloft when examining all models (Table 5). Using only those in the subset with lower RMS error scores against observations (which screens out the models with 2.7 and 11.2 day lifetimes, among others), the correlations increase at the surface in some cases, but decrease at 500 and 250 hPa. Even with the quality-screened subset of models, the residence time for regional emissions perturbations typically accounts for at most 20-50% of the variance in lower tropospheric Arctic sensitivities, and often 0-10%. Hence while variations in residence time account for a substantial fraction of the intermodel variance in Arctic sensitivities across all models,

they can explain only a modest portion of the variance in the subset. In the latter models, the variation in residence time is relatively small, so that processes such as wet removal of sulfate or in-cloud oxidation farther from the source region may be important in controlling how much sulfate reaches the Arctic even though they may not greatly affect the global residence time for regional emissions perturbations. Transport variations between models also play an important role for short-lived species, especially near the surface and in the upper troposphere (Table 6). Note that residence times are somewhat longer for European emissions, consistent with their larger impact on the Arctic. We also point out that sulfate changes are a function of both aerosol and oxidant precursor changes in these experiments, as precursors to both were changed simultaneously in the HTAP runs. This may at least partially explain why sulfate residence times are not as well correlated with Arctic sensitivities as are BC's. Hence diagnosing the physical processes responsible for the large spread in sulfate sensitivities will require much deeper investigation into model processes using additional diagnostics not available in the HTAP archive, and would benefit from additional simulations perturbing only aerosol precursors.

Overall, the comparison between the prescribed lifetime tracer and full chemistry simulations and the analyses of the correlation between residence times and Arctic concentrations both support the conclusion that dry transport differences among the models play a major role in the intermodel variations of insoluble, relatively long-lived CO. They are similarly important contributors to the model-to-model differences in mid-tropospheric ozone. However, these appear to be less important contributors to the intermodel variations in the Arctic sensitivity to aerosol emissions, for which uncertainties in aerosol physical and chemical processing, including wet removal, play the largest roles. Variations among models' Arctic cloud phase (ice versus liquid) and uncertainty about removal of aerosol by ice clouds may contribute to the large spread of aerosol results.

We also examined the relationship between horizontal resolution in the models and their representations of transport and of trace species in general. Horizontal resolution, using latitude, ranges from 1 to 5 degrees. We find R^2 correlations with resolution (using

latitude) to be extremely low for lifetimes and sensitivities. Hence there is no straightforward correlation with resolution.

6 Discussion and conclusions

The spread in model results for Arctic pollutants is very large for both gaseous species and aerosols. Differences in modeled transport, chemistry, removal and emissions all contribute to this spread, which makes climate and composition projections for the Arctic extremely challenging.

This study has identified the largest contributing factors to the diversity of model results. We have shown that for sulfate and BC (including deposition of the latter), uncertainties in modeling of aerosol physical and chemical processing are extremely important, with lesser roles for emissions and for dry transport. Further studies to determine precisely which physical processes play the largest role, such as those suggested by (Textor et al., 2006), would help prioritize research. In contrast, for CO, transport and emissions are important drivers of uncertainty in simulating surface responses to source region emissions, while transport, emissions and oxidation rates all play comparable roles at higher altitudes. For ozone, our analysis suggests that transport plays a substantial role in the intermodel variations in sensitivity, but that photochemical differences among the models appear to be the dominant contributor.

Our results for aerosols are consistent with earlier intercomparisons. These showed that the diversities in aerosol mass depend largely on differences in transport and the parameterizations of internal aerosol processes, and only to a lesser extent on their (precursor) emissions (Textor et al., 2007). These results held true for both the global aerosol load and the polar (>80° in both hemispheres) fraction. Our results also suggest that the contribution of intermodel dry transport differences to disparities in Arctic aerosol loading is relatively small, reinforcing the conclusion that aerosol and cloud physical and chemical processing (e.g. removal, oxidation and microphysics) is the principle source of uncertainty in modeling the distributions of these species in the Arctic. For realistic species whose lifetimes vary with location, transport and physical

processes are inherently coupled, however, and hence for the soluble aerosols these cannot be easily separated as sources of uncertainty.

For cases in which transport plays a substantial role in intermodel variability, such as CO or mid-tropospheric ozone, intercomparison among different models driven by the same meteorological fields would help determine the underlying reason for the range of results (complimenting studies of a single model driven by multiple meteorological fields, such as (Liu et al., 2007)). Differences in convection certainly contribute to transport variations among models. Model numerical schemes could also play a role, though algorithms such as conservation of second-order moments have been shown to generally transport trace species quite well, preserving gradients and not being too diffusive (Prather, 1986). However, this merits further study as many models may use less capable transport schemes. Additionally, the degree of agreement between chemical-transport models driven by offline meteorological fields and general circulation models that are relaxed towards offline meteorological fields remains to be characterized. Our comparison shows no clear effect of horizontal resolution.

Although the intermodel variations in transport to the Arctic are large, many of them are systematic across models so that differences between sensitivities to emissions from various regions are robust across models. In particular, we find that Arctic surface concentrations of BC, sulfate, and CO are substantially more sensitive to European emissions than to those from other regions. Similar results are obtained for the mid-troposphere (500 hPa), though the difference in sensitivities between Europe and other regions is not as large as for the surface. Hence per unit Tg emission change, European emissions are the most important for these species. We expect that Arctic sensitivities to emissions from Northern Asia would be generally similar to their European counterparts given the similarity in proximity and meteorological conditions.

The sensitivity of Arctic surface concentrations to European emissions maximizes during winter for CO, sulfate and BC. In the middle troposphere, sensitivity to European emissions is greatest in summer for aerosols. Sensitivity to East Asian emissions peaks during spring for BC, sulfate, and CO at both the surface and 500 hPa. Hence the relative importance of emissions from different regions varies seasonally. For surface ozone,

Arctic concentrations during summer are most sensitive to European emissions of NO_x, but sensitivities are comparable in fall for European and North American emissions, and in spring for East Asian, European and North American emissions. In the upper troposphere, concentrations for all species typically show comparable sensitivity to emissions from all four source regions, though there is a general tendency for a lower sensitivity to South Asian emissions (especially for CO).

The deposition of BC to the Arctic outside of Greenland is most sensitive to emissions from Europe in all seasons. In contrast, deposition of BC to Greenland is most sensitive to North American emissions, except during winter when sensitivity to European emissions becomes comparable. Total deposition of BC, rather than per unit emission, is again greater from Europe than the other regions for the Arctic exclusive of Greenland. Annual mean total BC deposition onto Greenland is greatest from North America and Europe, which are nearly equal, with a substantial but lesser contribution from East Asia. These conclusions are robust across the models examined here. Total springtime deposition to Greenland is primarily due to emissions from North America and East Asia, when Greenland is less affected by European emissions than in other seasons. As springtime deposition appears to be especially effective in inducing large snow-albedo feedbacks (Flanner et al., 2007), this suggests an enhanced role in Greenland climatic forcing for East Asian and North American emissions relative to their annual mean contribution to deposition.

The recent recovery of ice core records from Greenland containing BC (McConnell et al., 2007) may allow better estimates of historical BC emissions. The results presented here indicate that even without including Russian emissions, North America is responsible for less than half the BC deposition onto Greenland (Table 4). Hence the ice core record may indeed reflect very large emissions during the early 20th century from Eastern North America (McConnell et al., 2007), but it could also include the effects of historical emissions from other regions. Analysis of variations in deposition across Greenland might help clarify this issue, as could further analysis of historical emission trends by matching the onset and duration of the early 20th century BC deposition maximum seen in the ice core record.

Previous work has discussed apparently conflicting results on transport of BC to the Arctic (Law and Stohl, 2007). The results of (Koch and Hansen, 2005) indicated that Arctic BC optical thickness results mostly from Asian emissions (excluding Russia, so roughly corresponding to our SA+EA). Impacts from European and North American emissions were roughly half to one-third of the Asian ones, and Asian emissions also played a major role in the low altitude springtime Arctic Haze. In contrast, (Stohl, 2006) found that transport from Europe to the Arctic surface was much more effective than from South and East Asia. The mean BC emissions in HTAP are: SA 0.87, EA 1.80, NA 0.66, EU 0.93 Tg yr^{-1}. In (Koch and Hansen, 2005), they are: SA+EA 2.08, EU 0.47, NA 0.39 Tg yr^{-1}. Using either set of emissions and the mean or median sensitivities found here, BC in the upper troposphere is indeed dominated by Asian emissions (as in Table 3). In the mid-troposphere, Asian emissions dominate during spring, have comparable impact to European emissions in winter and fall, and are less important in summer using HTAP emissions (seasonal results are given in the Auxiliary material). Using those of (Koch and Hansen, 2005), Asian emissions would be most important in all seasons. Examining springtime low altitude BC pollution (contributing to Arctic Haze), Asian sources contribute 57% as much as European sources in the HTAP models to BC at the surface, and 134% as much at 500 hPa (multi-model means). Again, using the HTAP sensitivities and the Koch and Hansen (2005) emissions, Asian sources would contribute more strongly to Arctic BC. Hence although the GISS model used by (Koch and Hansen, 2005) transports BC to the Arctic more efficiently than other models (though apparently in better agreement with observations (Figure 7)), their results for the relative importance of emissions from different regions are generally similar to the mean BC model simulations analyzed here, with differences largely arising from the differing emission inventories used. The large contribution of Asian BC emissions contrasts with the results of Stohl (2006), who found Asian contributions to springtime Arctic surface BC to be only about 10% of European contributions (using the same emissions inventory as Koch and Hansen (2005)). We find no contradiction, however, between the large impacts of Asian BC aloft in the Arctic and the dominant role of European emissions on surface BC.

The differences between the results of Stohl (2006) and the HTAP models may relate to the Langrangian setup of the former, while the latter models are Eulerian. This could lead

to different representations of transport pathways in the models. To examine this, we have calculated the mean and standard deviation of the relative contribution of emissions from each region to the total BC response to perturbations (Figures 9 and 10). The HTAP models show the largest contribution from European emissions to the European and Russian portion of the Arctic while East Asian emissions have their largest relative contribution in the Siberian and North American portions. Standard deviations across models are typically largest around the boundaries of the regions with greatest relative contribution. This suggests that much of the variability results from the differing residence times of BC, which allows transport over a longer or shorter distance (consistent with the high correlations between Arctic BC and residence time discussed in section 5.2). Hence these standard deviations are often fairly uniform, such as those around the edges of the areas of maximum European contribution in winter or of maximum North American contribution in summer. However, there are also distinct areas of larger standard deviation that do suggest intermodel variations in transport along particular paths. These include summer transport from Asia across the pole to Greenland, from North America to Siberia, and to some extent cross-polar transport from Europe to North America, and during winter, westward transport from North America across Siberia. At upper levels, standard deviations are typically smoother. Overall, the Eulerian models do not appear to show transport pathways to the Arctic that are remarkably different from one another, however. We believe that the discrepancy between the HTAP models and the results of Stohl (2006) is therefore most likely due to a fundamental difference between the Eulerian and the Langrangian setup, such as differences in diffusion, or to the lack of removal processes in the Langrangian parcel model study.

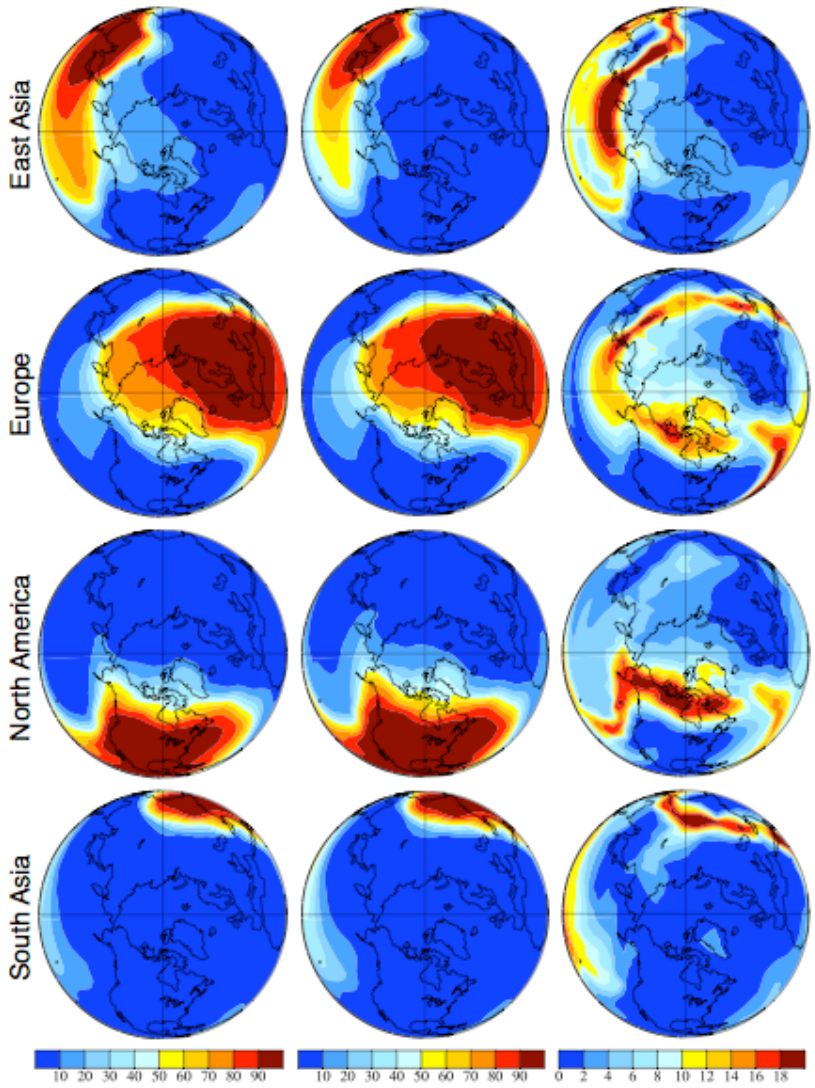

Figure 9. Relative contribution of regional emissions to winter Arctic surface BC. Values are the relative contribution (%) to the total response to emissions from the four source regions (left column), the relative contribution (%) per unit source region emission (center column), and the standard deviation of the latter across the HTAP models (right column). Results are based on 8 models (three models with small-spatial scale structure were excluded from these calculations for clarity).

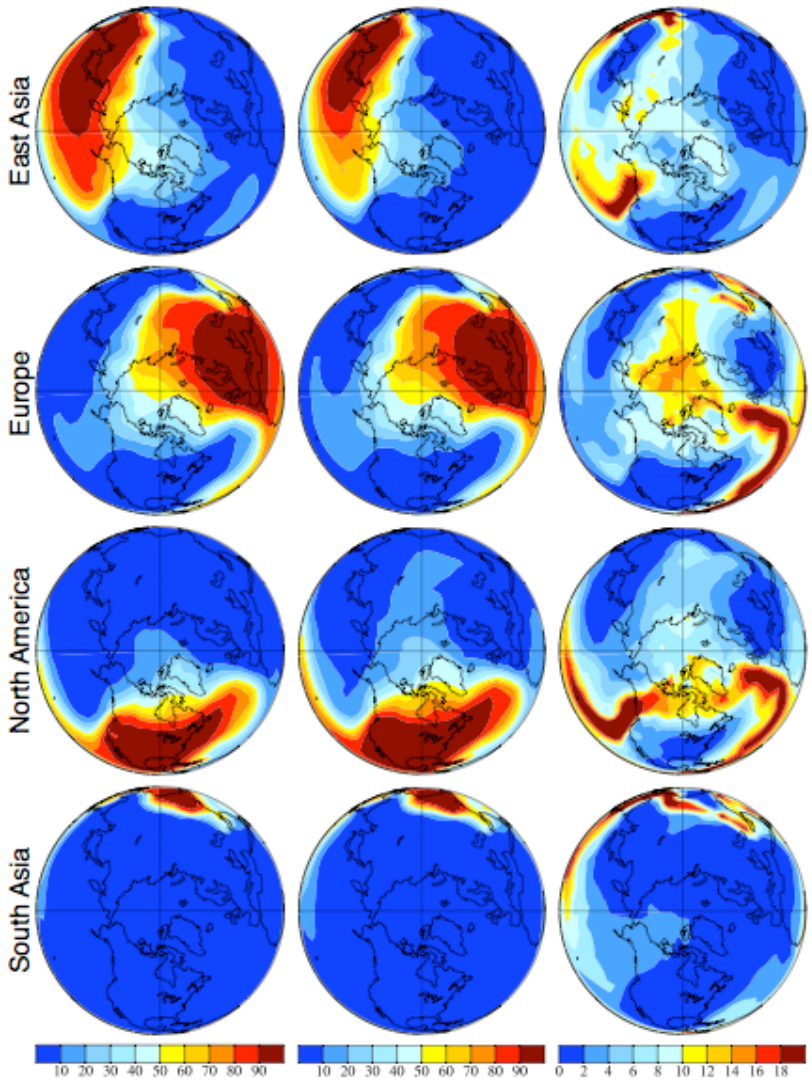

Figure 10. As Figure 9 but for summer.

The results presented here help to characterize the relative importance of emissions from various source regions to seasonal and annual Arctic pollution. It remains an open question how these sensitivities may change in the future. As climate continues to change, Arctic temperatures are projected to increase faster than those at lower latitudes. This would reduce the temperature difference between the Arctic and pollution source regions, enhancing low-altitude transport of pollution into the Arctic. This might lead to increased pollutant concentrations and, if these were primarily climate warming agents, a further increase in surface temperatures. Additionally, large-scale circulation patterns are also projected to respond to climate change. These may respond to the projected increase

in the temperature gradient in the vicinity of the tropopause rather than the decreased gradient near the surface (Shindell et al., 2001). The Arctic may be strongly affected by changes in the Northern Hemisphere westerlies associated with the North Atlantic Oscillation/Northern Annular Mode (Eckhardt et al., 2003; Duncan and Bey, 2004), which are projected to accelerate in the future (Miller et al., 2006). These westerlies have been shown to substantially enhance pollutant transport to the Arctic, at least from some regions (Sharma et al., 2006). Hence transport from highly polluted source regions may become more frequent in the future.

At the same time, emissions will also be changing. Projected increases from East Asia would be especially effective in causing more springtime ozone, sulfate, BC and CO both at the Arctic surface and in the mid-troposphere. Reductions in emissions from developed nations in North America and Europe would cause decreases in surface level CO and BC that would be especially pronounced in winter. This would also substantially reduce BC deposition onto Greenland, though the reduction might be largely offset, especially during spring and summer, by Asian emission increases. Surface sulfate would be reduced year-round with decreased emissions from industrialized countries, while ozone concentrations would decrease most in non-winter seasons. Hence changes in the seasonal cycle of surface CO and BC, for example, with a reduced winter-to-spring gradient, could result from a shift in emissions from the developed to the developing world. Emissions might also increase within the Arctic itself, with large potential impacts on local pollutant concentrations.

Understanding of future Arctic pollution levels will require simulations incorporating both changing climate and emissions. Our confidence in the results of such simulations could be greatly improved by resolving some of the apparent discrepancies between model results and observations, especially for aerosols. Additional measurements of Arctic sulfate and BC aerosols would be helpful to provide additional model constraints. For example, the BC data from Alert and Barrow, both in the Western Hemisphere, can clearly not be expected to be representative of the Arctic as a whole given the different impact of regional emissions on the Eastern and Western Hemisphere portions of the Arctic (Figures 9 and 10). Better understanding of the mass absorption efficiency of BC and other absorbing species would also be useful. Hopefully the activities of the

International Polar Year 2007-2009 will substantially increase our knowledge of the Arctic, and a hightened focus on the Arctic by the scientific community will lead to at least some of these measurements being maintained over the long-term. Nevertheless, the current results are robust across models in many respects, allowing better understanding of how various types of pollutants arrive in the Arctic and influence climate and air quality.

Acknowledgements

We thank the NASA Atmospheric Chemistry Modeling and Analysis Program for support, and D. Henze for comments. MGS and KJP were funded by the UK Defra under contract AQ0409, and were also supported by the Joint Defra and MoD Programme, (Defra) GA01101 (MoD) CBC/2B/0417_Annex C5. This work was performed under the umbrella of the Task Force - Hemispheric Transport of Air Pollution (www.htap.org). This work performed under the auspices of the U.S. Department of Energy by Lawrence Livermore National Laboratory under Contract DE-AC52-07NA27344.

References

Bodhaine, B. A.: Aerosol absorption measurements at barrow, mauna loa and the south pole, J. Geophys. Res., 100, 8967 – 8976, 1995.

Duncan, B. N., and Bey, I.: A modeling study of the export pathways of pollution from europe: Seasonal and interannual variations (1987–1997), J. Geophys. Res., 109, D08301, doi:10.1029/2003JD004079, 2004.

Eckhardt , S., Stohl, A., Beirle, S., Spichtinger, N., James, P., Forster, C., Junker, C., Wagner, T., Platt, U., and Jennings, S. G.: The north atlantic oscillation controls air pollution transport to the arctic, Atmos. Chem. Phys., 3, 1769-1778, 2003.

Flanner, M. G., Zender, C. S., Randerson, J. T., and Rasch, P. J.: Present-day climate forcing and response from black carbon in snow, J. Geophys. Res., 112, D11202, doi:10.1029/2006JD008003, 2007.

Garrett, T. J., and Zhao, C.: Increased arctic cloud longwave emissivity associated with pollution from mid-latitudes, Nature, 440, 787-789, 2006.

Hansen, J., and Nazarenko, L.: Soot climate forcing via snow and ice albedos, Proc. Natl. Acad. Sci., 101, 423-428, doi:410.1073/pnas.2237157100, 2004.

Hjellbrekke, A.-G., and Fjæraa, A. M.: Data report 2005 acidifying and eutrophying compounds, and particulate matter, EMEP/CCC-Report 1/2007, 2007.

Jacobson, M. Z.: Climate response of fossil fuel and biofuel soot, accounting for soot's feedback to snow and sea ice albedo and emissivity J. Geophys. Res., 109, D21201, doi:10.1029/2004JD004945, 2004.

Klonecki, A., Hess, P., Emmons, L., Smith, L., Orlando, J., and Blake, D.: Seasonal changes in the transport of pollutants into the arctic troposphere-model study, J. Geophys. Res., 108, 8367, doi:10.1029/2002JD002199, 2003.

Koch, D., and Hansen, J.: Distant origins of arctic black carbon: A goddard institute for space studies modele experiment, J. Geophys. Res., 110, D04204, doi:10.1029/2004JD005296, 2005.

Law, K. S., and Stohl, A.: Arctic air pollution: Origins and impacts, Science, 315, 1537-1540, 2007.

Liu, X., Penner, J. E., Das, B., Bergmann, D., Rodriguez, J. M., Strahan, S., Wang, M., and Feng, Y.: Uncertainties in global aerosol simulations: Assessment using three

meteorological datasets, J. Geophys. Res., 112, D11212, doi:10.1029/2006JD008216, 2007.
Lubin, D., and Vogelmann, A. M.: A climatologically significant aerosol longwave indirect effect in the arctic, Nature, 439, 453-456, 2006.
McConnell, J., Edwards, R., Kok, G., Flanner, M., Zender, C., Saltzman, E., Banta, J., Pasteris, D., Carter, M., and Kahl, J.: 20th-century industrial black carbon emissions altered arctic climate forcing, Science, 317, 1381-1384, 2007.
Miller, R. L., Schmidt, G. A., and Shindell, D. T.: Forced variations of annular modes in the 20th century intergovernmental panel on climate change fourth assessment report models, J. Geophys. Res., 111, D18101, doi:10.1029/2005JD006323, 2006.
Novelli, P. C., Masarie, K. A., and Lang, P. M.: Distributions and recent changes in carbon monoxide in the lower troposphere, J. Geophys. Res., 103, 19015- 19033, 1998.
Oltmans, S. J., and Levy, H.: Surface ozone measurements from a global network, Atmos. Env., 28, 9-24, 1994.
Park, R. J., Jacob, D. J., Palmer, P. I., Clarke, A. D., Weber, R. J., Zondlo, M. A., Eisele, F. L., Bandy, A. R., Thornton, D. C., Sachse, G. W., and Bond, T. C.: Export efficiency of black carbon aerosol in continental outflow: Global implications, J. Geophys. Res., 110, D11205, doi:10.1029/2004JD005432, 2005.
Prather, M. J.: Numerical advection by conservation of second-order moments, J. Geophys. Res., 91, 6671-6681, 1986.
Quinn, P. K., Bates, T. S., Baum, E., Doubleday, N., Fiore, A. M., Flanner, M., Fridlind, A., Garrett, T. J., Koch, D., Menon, S., Shindell, D., Stohl, A., and Warren, S. G.: Short-lived pollutants in the arctic: Their climate impact and possible mitigation strategies, Atmos. Chem. Phys., 8, 1723-1735, 2007.
Sharma, S., Andrews, E., Barrie, L. A., Ogren, J. A., and Lavoué, D.: Variations and sources of the equivalent black carbon in the high arctic revealed by long-term observations at alert and barrow: 1989–2003, J. Geophys. Res., 111, D14208, doi:10.1029/2005JD006581, 2006.
Shindell, D.: Local and remote contributions to arctic warming, Geophys. Res. Lett., 34, L14704, doi:10.1029/2007GL030221, 2007.

Shindell, D. T., Schmidt, G. A., Miller, R. L., and Rind, D.: Northern hemisphere winter climate response to greenhouse gas, volcanic, ozone and solar forcing, J. Geophys. Res., 106, 7193-7210, 2001.
Shindell, D. T., Faluvegi, G., Stevenson, D. S., Krol, M. C., Emmons, L. K., Lamarque, J.-F., Petron, G., Dentener, F. J., Ellingsen, K., Schultz, M. G., Wild, O., Amann, M., Atherton, C. S., Bergmann, D. J., Bey, I., Butler, T., Cofala, J., Collins, W. J., Derwent, R. G., Doherty, R. M., Drevet, J., Eskes, H. J., Fiore, A. M., Gauss, M., Hauglustaine, D. A., Horowitz, L. W., Isaksen, I. S. A., Lawrence, M. G., Montanaro, V., Muller, J. F., Pitari, G., Prather, M. J., Pyle, J. A., Rast, S., Rodriguez, J. M., Sanderson, M. G., Savage, N. H., Strahan, S. E., Sudo, K., Szopa, S., Unger, N., van Noije, T. P. C., and Zeng, G.: Multi-model simulations of carbon monoxide: Comparison with observations and projected near-future changes, J. Geophys. Res., 111, D19306, doi:10.1029/2006JD007100, 2006.
Sirois, A., and Barrie, L. A.: Arctic lower tropospheric aerosol trends and composition at alert, canada: 1980–1995, J. Geophys. Res., 104, 11,599–511,618, 1999.
Stohl, A.: Characteristics of atmospheric transport into the arctic troposphere, J. Geophys. Res., 111, D11306, doi:10.1029/2005JD006888, 2006.
Textor, C., Schulz, M., Guibert, S., Kinne, S., Balkanski, Y., Bauer, S., Berntsen, T., Berglen, T., Boucher, O., Chin, M., Dentener, F., Diehl, T., Easter, R., Feichter, H., Fillmore, D., Ghan, S., Ginoux, P., Gong, S., Grini, A., Hendricks, J., Horowitz, L., Huang, P., Isaksen, I. S. A., Iversen, T., Kloster, S., Koch, D., Kirkevåg, A., Kristjansson, J. E., Krol, M., Lauer, A., Lamarque, J. F., Liu, X., Montanaro, V., Myhre, G., Penner, J. E., Pitari, G., Reddy, M. S., Seland, Ø., Stier, P., Takemura, T., and Tie, X.: Analysis and quantification of the diversities of aerosol life cycles within aerocom, Atmos. Chem. Phys., 6, 1777-1813, 2006.
Textor, C., Schulz, M., Guibert, S., Kinne, S., Balkanski, Y., Bauer, S., Berntsen, T., Berglen, T., Boucher, O., Chin, M., Dentener, F., Diehl, T., Feichter, H., Fillmore, D., Ginoux, P., Gong, S., Grini, A., Hendricks, J., Horowitz, L., Huang, P., Isaksen, I. S. A., Iversen, T., Kloster, S., Koch, D., Kirkevåg, A., Kristjansson, J. E., Krol, M., Lauer, A., Lamarque, J. F., Liu, X., Montanaro, V., Myhre, G., Penner, J. E., Pitari, G., Reddy, M. S., Seland, Ø., Stier, P., Takemura, T., and Tie, X.: The effect of harmonized emissions

on aerosol properties in global models – an aerocom experiment, Atmos. Chem. Phys., 7, 4489-4501, 2007.
Vogelmann, A. M., Robock, A., and Ellingson, R. G.: Effects of dirty snow in nuclear winter simulations, J. Geophys. Res., 93, 5319-5332, 1988.
Warren, S. G., and Wiscombe, W. J.: A model for the spectral albedo of snow. Ii: Snow containing atmospheric aerosols, J. Atmos. Sci., 37, 2734-2745, 1980.
Xie, Y.-L., Hopke, P. K., Paatero, P., Barrie, L. A., and Li, S.-M.: Identification of source nature and seasonal variations of arctic aerosol by positive matrix factorization, J. Atmos. Sci., 56, 249–260, 1999.

Table 1. Models simulations used in the analyses

Model	Gas-phase	Aerosols	Prescribed lifetime	Horizontal Resolution
1. CAMCHEM	NOx, CO	SO2, BC	Y	1.9
2. ECHAM5-HAMMOZ		SO2, BC		2.8
3. EMEP	NOx, CO	SO2		1.0
4. FRSGC/UCI	NOx, CO		Y	2.8
5. GEOSChem	NOx	SO2, BC		2.0
6. GISS-PUCCINI	NOx, CO	SO2, BC	Y	4.0
7. GMI	NOx, CO	SO2, BC	Y	2.0
8. GOCART-2		SO2, BC		2.0
9. LMDz4-INCA		SO2, BC		2.5
10. LLNL-IMPACT	NOx, CO	SO2, BC		2.0
11. MOZARTGFDL	NOx, CO	SO2, BC	Y	1.9
12. MOZECH	NOx, CO		Y	2.8
13. SPRINTARS		SO2, BC		1.1
14. STOCHEM-HadGEM1	NOx, CO			3.8
15. STOCHEM-HadAM3	NOx, CO	SO2	Y	5.0
16. TM5-JRC	NOx	SO2, BC		1.0
17. UM-CAM	NOx, CO		Y	2.5

The response to perturbations in emissions of the indicated species were simulated by the models listing those species. Prescribed lifetime indicates that an additional simulation with idealized prescribed lifetime tracers was also performed. Note that a few models did not perform all the regional perturbation experiments. Horizontal resolution is in degrees latitude.

Table 2. Mean (max, min) of total emissions in each region in Tg/yr across all models in their base run

	S in SO_2	BC	CO	N in NO_x
East Asia	17 (21, 16)	1.8 (2.1, 1.5)	156 (220, 128)	7.0 (10.8, 5.2)
Europe	18 (25, 15)	0.9 (2.1, 0.7)	90 (130, 70)	8.4 (9.7, 7.2)
North America	11 (15, 10)	0.7 (0.9, 0.5)	129 (154, 107)	8.7 (9.4, 7.7)
South Asia	4 (5, 4)	0.9 (1.4, 0.6)	98 (145, 74)	3.3 (4.2, 2.6)

NO_x=NO+NO_2

Table 3. Annual average Arctic absolute mixing ratio decreases due to 20% reductions in anthropogenic emissions in each region

	EA	EU	NA	SA
Surface				
Sulfate (pptm)	2.16 ± 1.92 (13%)	12.4 ± 9.8 (73%)	2.27 ± 1.97 (13%)	0.20 ± 0.23 (1%)
	1.87 (13%)	10.0 (71%)	2.03 (15%)	0.09 (1%)
BC (pptm)	0.18 ± 0.22 (17%)	0.77 ± 0.75 (72%)	0.11 ± 0.11 (10%)	0.01 ± 0.02 (1%)
	0.10 (16%)	0.47 (74%)	0.05 (8%)	0.01 (2%)
CO (ppbv)	2.23 ± 1.07 (26%)	3.35 ± 1.12 (39%)	2.42 ± 0.75 (29%)	0.51 ± 0.15 (6%)
	1.8 (24%)	2.84 (37%)	2.42 (32%)	0.51 (7%)
Ozone (ppbv)	0.12 ± 0.04 (27%)	0.11 ± 0.07 (24%)	0.19 ± 0.07 (42%)	0.02 ± 0.01 (7%)
	0.11 (24%)	0.13 (28%)	0.20 (43%)	0.02 (4%)
500 hPa				
Sulfate (pptm)	11.4 ± 10.4 (25%)	23.3 ± 20.3 (51%)	9.83 ± 9.09 (21%)	1.32 ± 1.78 (3%)
	10.6 (25%)	22.9 (53%)	9.16 (21%)	0.53 (1%)
BC (pptm)	0.91 ± 0.95 (38%)	0.97 ± 0.99 (41%)	0.41 ± 0.41 (17%)	0.10 ± 0.13 (4%)
	0.75 (43%)	0.68 (39%)	0.26 (15%)	0.05 (3%)
CO (ppbv)	2.38 ± 1.01 (31%)	2.20 ± 0.54 (28%)	2.52 ± 0.71 (33%)	0.61 ± 0.17 (8%)
	1.88 (26%)	2.11 (30%)	2.43 (34%)	0.68 (10%)
Ozone (ppbv)	0.26 ± 0.09 (23%)	0.35 ± 0.11 (31%)	0.44 ± 0.15 (40%)	0.07 ± 0.05 (6%)
	0.24 (22%)	0.39 (36%)	0.40 (37%)	0.05 (5%)
250 hPa				
Sulfate (pptm)	17.4 ± 16.4 (36%)	14.6 ± 14.1 (30%)	11.3 ± 11.6 (24%)	4.68 ± 5.38 (10%)
	15.6 (41%)	11.8 (31%)	7.93 (21%)	2.42 (7%)
BC (pptm)	1.16 ± 1.08 (48%)	0.45 ± 0.40 (18%)	0.36 ± 0.33 (15%)	0.47 ± 0.50 (19%)
	0.75 (47%)	0.34 (21%)	0.23 (15%)	0.27 (17%)
CO (ppbv)	1.35 ± 0.48 (36%)	0.77 ± 0.21 (20%)	1.11 ± 0.28 (29%)	0.58 ± 0.23 (16%)
	1.28 (35%)	0.70 (19%)	1.14 (31%)	0.57 (15%)
Ozone (ppbv)	0.22 ± 0.01 (25%)	0.22 ± 0.17 (25%)	0.35 ± 0.19 (39%)	0.10 ± 0.07 (11%)
	0.21 (25%)	0.18 (22%)	0.35 (42%)	0.09 (11%)

For each species, values in the first row are multi-model means and standard deviations, while values in the second row are medians. The percentage of the total from these four source regions for each individual region is given in parentheses for both mean and median values. Ozone and sulfate changes are in response to NO_x and SO_2 emissions changes, respectively.

Table 4. Annual average BC deposition to Greenland and Arctic excluding Greenland ($Tg/m^2 \times 10^{-14}$) due to 20% of anthropogenic emissions from each region

	EA	EU	NA	SA
Greenland				
All models	0.7 ± 1.0	1.4 ± 1.7	1.5 ± 1.8	0.10 ± 0.14
Excluding largest	0.5 ± 0.4	1.1 ± 1.3	1.1 ± 1.2	0.06 ± 0.04
Excluding smallest	0.8 ± 1.0	1.5 ± 1.7	1.7 ± 1.9	0.11 ± 0.14
Arctic (excluding Greenland)				
All models	22 ± 29	80 ± 94	13 ± 17	2.2 ± 3.9
Excluding largest	13 ± 10	59 ± 70	8.7 ± 8.6	1.0 ± 0.6
Excluding smallest	24 ± 30	88 ± 96	15 ± 17	2.4 ± 4.1

Values are multi-model means and standard deviations.

Table 5. Lifetime or residence time (days) and correlation coefficients (R^2) between those times and Arctic sensitivity across the models

		EA	EU	NA	SA
CO subset	Surface correlation	.0	.3	.1	.8
(Global mean	500 hPa correlation	.0	.0	.0	.8
lifetime 62 ± 12)	250 hPa correlation	.3	.3	.4	.6
CO all	Surface correlation	.3	.0	.3	.9
(Global mean	500 hPa correlation	.4	.2	.3	.9
lifetime 57 ± 15)	250 hPa correlation	.4	.4	.5	.4
BC all	Mean residence time	4.9 ± 2.0	5.8 ± 1.4	5.1 ± 1.5	6.6 ± 1.5
	Surface correlation	.8	.8	.8	.2
	500 hPa correlation	.8	.7	.8	.3
	250 hPa correlation	.9	.6	.8	.4
SO_4 subset	Mean residence time	4.8 ± 0.9	7.0 ± 1.9	4.7 ± 0.9	5.6 ± 1.2
	Surface correlation	.2	.0	.5	.8
	500 hPa correlation	.0	.0	.1	.5
	250 hPa correlation	.2	.0	.3	.1
SO_4 all	Mean residence time	4.3 ± 1.9	6.1 ± 2.2	4.7 ± 2.1	5.3 ± 2.5
	Surface correlation	.2	.1	.1	.1
	500 hPa correlation	.5	.4	.5	.5
	250 hPa correlation	.6	.3	.7	.4

Global mean multimodel means and standard deviations of residence times for regional emissions for aerosols and global mean chemical lifetime from the control run for CO are given. R^2 values are linear correlations between those times and the Arctic sensitivities at the given pressure levels. "All" and "subset" refer to the models used in the analysis (see text for subsets). The EMEP model was excluded since it includes the NH only and hence its global lifetime is not precisely equivalent to the others. In the CO analysis, GMI and MOZECH were not included due to problematic diagnostics.

Table 6. Standard deviations of annual mean Arctic values of prescribed lifetime tracers across models (%)

	surface	500 hPa	250 hPa
5.6 day VOC	19.7	6.4	14.0
13 day VOC	18.2	5.6	7.9
64 day VOC	9.7	3.9	6.0
50 day CO	7.5	6.9	7.8
50 day soluble CO	62.6	65.7	76.7

The three VOC-like tracers used identical VOC emissions, while the two CO-like tracers used CO emissions. Hence comparison within the VOC subset shows the effect of lifetime changes, comparison of the two CO tracers shows the effect of solubility, and differences between the 64 day VOC and 50 day CO are mostly due to differing emissions.

Auxiliary material

Table A1. Arctic average absolute mixing ratio decreases due to 20% reductions in anthropogenic emissions in each region for the four seasons

Dec-Jan

	EA	EU	NA	SA
Surface				
Sulfate (pptm)	1.33 ± 1.38 (8%)	14.1 ± 12.4 (80%)	1.90 ± 2.07 (10%)	0.31 ± 0.41 (2%)
BC (pptm)	0.12 ± 0.19 (7%)	1.44 ± 1.55 (86%)	0.10 ± 0.12 (6%)	0.02 ± 0.04 (1%)
CO (ppbv)	2.22 ± 1.01 (21%)	4.97 ± 2.07 (47%)	2.90 ± 0.75 (27%)	0.56 ± 0.12 (5%)
Ozone (ppbv)	0.13 ± 0.05 (26%)	0.14 ± 0.22 (28%)	0.18 ± 0.07 (36%)	0.05 ± 0.02 (10%)
500 hPa				
Sulfate (pptm)	5.45 ± 5.47 (25%)	9.6 ± 10.3 (43%)	5.89 ± 6.10 (27%)	1.20 ± 1.40 (5%)
BC (pptm)	0.57 ± 0.71 (35%)	0.59 ± 0.63 (37%)	0.32 ± 0.35 (20%)	0.13 ± 0.15 (8%)
CO (ppbv)	2.61 ± 1.09 (29%)	2.61 ± 0.70 (29%)	3.07 ± 0.67 (34%)	0.68 ± 0.15 (8%)
Ozone (ppbv)	0.21 ± 0.06 (30%)	0.12 ± 0.07 (17%)	0.29 ± 0.09 (42%)	0.08 ± 0.03 (11%)
250 hPa				
Sulfate (pptm)	10.2 ± 10.5 (38%)	5.23 ± 6.25 (19%)	7.39 ± 9.34 (27%)	4.25 ± 5.62 (16%)
BC (pptm)	0.70 ± 0.73 (47%)	0.17 ± 0.18 (11%)	0.24 ± 0.26 (16%)	0.39 ± 0.38 (26%)
CO (ppbv)	1.32 ± 0.43 (34%)	0.74 ± 0.25 (19%)	1.19 ± 0.29 (31%)	0.58 ± 0.25 (15%)
Ozone (ppbv)	0.16 ± .10 (26%)	0.12 ± 0.12 (19%)	0.25 ± 0.18 (40%)	0.09 ± 0.06 (15%)

Mar-May

	EA	EU	NA	SA
Surface				
Sulfate (pptm)	3.84 ± 3.79 (19%)	13.4 ± 13.2 (65%)	3.04 ± 3.25 (15%)	0.22 ± 0.30 (1%)
BC (pptm)	0.30 ± 0.38 (31%)	0.52 ± 0.51 (54%)	0.13 ± 0.14 (13%)	0.02 ± 0.03 (2%)
CO (ppbv)	3.17 ± 1.54 (29%)	4.04 ± 1.44 (36%)	3.11 ± 0.93 (28%)	0.76 ± 0.30 (7%)
Ozone (ppbv)	0.17 ± 0.06 (28%)	0.18 ± 0.07 (30%)	0.21 ± 0.07 (35%)	0.04 ± 0.01 (7%)
500 hPa				

Sulfate (pptm)	18.3 ± 16.7 (30%)	29.2 ± 27.0 (48%)	11.6 ± 10.9 (19%)	1.92 ± 2.28 (3%)
BC (pptm)	1.48 ± 1.49 (47%)	1.10 ± 1.14 (35%)	0.44 ± 0.46 (14%)	0.15 ± 0.17 (4%)
CO (ppbv)	3.20 ± 1.42 (32%)	2.85 ± 0.83 (29%)	3.02 ± 0.83 (30%)	0.90 ± 0.31 (9%)
Ozone (ppbv)	0.30 ± 0.08 (24%)	0.42 ± 0.13 (34%)	0.45 ± 0.14 (36%)	0.07 ± 0.03 (6%)
250 hPa				
Sulfate (pptm)	14.8 ± 12.3 (35%)	12.9 ± 15.0 (30%)	9.20 ± 9.09 (22%)	5.49 ± 5.50 (13%)
BC (pptm)	0.94 ± 0.82 (46%)	0.37 ± 0.38 (18%)	0.29 ± 0.31 (14%)	0.46 ± 0.42 (22%)
CO (ppbv)	1.39 ± 0.49 (35%)	0.77 ± 0.28 (19%)	1.09 ± 0.31 (27%)	0.73 ± 0.32 (18%)
Ozone (ppbv)	0.18 ± 0.13 (23%)	0.20 ± 0.19 (26%)	0.30 ± 0.21 (38%)	0.10 ± 0.06 (13%)

Jun-Aug

	EA	EU	NA	SA
Surface				
Sulfate (pptm)	2.17 ± 1.99 (14%)	10.5 ± 7.3 (70%)	2.30 ± 1.77 (15%)	0.12 ± 0.17 (1%)
BC (pptm)	0.17 ± 0.17 (25%)	0.40 ± 0.26 (60%)	0.09 ± 0.08 (13%)	0.01 ± 0.01 (2%)
CO (ppbv)	1.96 ± 1.21 (34%)	1.70 ± 0.78 (29%)	1.73 ± 0.93 (30%)	0.43 ± 0.21 (7%)
Ozone (ppbv)	0.07 ± 0.03 (18%)	0.19 ± 0.08 (49%)	0.13 ± 0.09 (33%)	0.00 ± 0.01 (0%)
500 hPa				
Sulfate (pptm)	12.6 ± 14.1 (22%)	31.8 ± 28.8 (56%)	11.3 ± 10.9 (20%)	1.14 ± 2.00 (2%)
BC (pptm)	0.75 ± 0.78 (31%)	1.21 ± 1.23 (50%)	0.40 ± 0.36 (17%)	0.06 ± 0.08 (2%)
CO (ppbv)	1.82 ± 1.02 (33%)	1.56 ± 0.57 (28%)	1.75 ± 0.90 (31%)	0.46 ± 0.23 (8%)
Ozone (ppbv)	0.21 ± 0.09 (17%)	0.50 ± 0.19 (42%)	0.47 ± 0.22 (39%)	0.02 ± 0.02 (2%)
250 hPa				
Sulfate (pptm)	24.1 ± 22.4 (37%)	23.8 ± 22.7 (36%)	14.1 ± 12.4 (22%)	3.56 ± 3.71 (5%)
BC (pptm)	1.51 ± 1.42 (48%)	0.79 ± 0.65 (25%)	0.46 ± 0.40 (15%)	0.39 ± 0.49 (12%)
CO (ppbv)	1.39 ± 0.65 (36%)	0.88 ± 0.28 (23%)	1.08 ± 0.38 (28%)	0.51 ± 0.28 (13%)
Ozone (ppbv)	0.26 ± 0.15 (24%)	0.35 ± 0.22 (32%)	0.42 ± 0.24 (38%)	0.07 ± 0.05 (6%)

Sep-Nov

	EA	EU	NA	SA
Surface				

Sulfate (pptm)	1.27 ± 1.14 (9%)	11.6 ± 10.5 (78%)	1.84 ± 1.55 (12%)	0.14 ± 0.17 (1%)
BC (pptm)	0.11 ± 0.16 (12%)	0.75 ± 0.78 (77%)	0.10 ± 0.12 (10%)	0.01 ± 0.01 (1%)
CO (ppbv)	1.54 ± 0.93 (24%)	2.65 ± 0.92 (41%)	1.93 ± 0.95 (30%)	0.30 ± 0.16 (5%)
Ozone (ppbv)	0.10 ± 0.04 (18%)	0.21 ± 0.08 (38%)	0.23 ± 0.10 (42%)	0.01 ± 0.01 (2%)
500 hPa				
Sulfate (pptm)	8.95 ± 8.86 (21%)	22.3 ± 21.9 (52%)	10.5 ± 10.9 (25%)	1.00 ± 1.59 (2%)
BC (pptm)	0.81 ± 0.85 (35%)	0.94 ± 1.04 (41%)	0.46 ± 0.50 (20%)	0.08 ± 0.10 (4%)
CO (ppbv)	1.88 ± 0.92 (30%)	1.85 ± 0.47 (29%)	2.25 ± 0.90 (35%)	0.39 ± 0.19 (6%)
Ozone (ppbv)	0.24 ± 0.07 (21%)	0.36 ± 0.12 (32%)	0.48 ± 0.18 (43%)	0.05 ± 0.03 (4%)
250 hPa				
Sulfate (pptm)	20.2 ± 22.5 (36%)	16.1 ± 16.6 (28%)	14.5 ± 16.5 (26%)	5.42 ± 7.22 (10%)
BC (pptm)	1.49 ± 1.62 (49%)	0.48 ± 0.43 (16%)	0.46 ± 0.44 (15%)	0.63 ± 0.80 (20%)
CO (ppbv)	1.30 ± 0.52 (37%)	0.67 ± 0.21 (19%)	1.06 ± 0.32 (30%)	0.51 ± 0.24 (14%)
Ozone (ppbv)	0.26 ± 0.14 (25%)	0.25 ± 0.17 (25%)	0.41 ± 0.21 (40%)	0.10 ± 0.07 (10%)

For each species, values are multi-model means and standard deviations. The percentage of the total from these four source regions for each individual region is given in parentheses. Ozone and sulfate changes are in response to NO_x and SO_2 emissions changes, respectively.